UNIVERSITY OF CALIFORNIA
RIVERSIDE

Percolation Transitions on Finite Transitive Hyperbolic Graphs

A Dissertation submitted in partial satisfaction
of the requirements for the degree of

Doctor of Philosophy

in

Physics

by

Michael Dean Woolls

December 2020

Dissertation Committee:

Dr. Leonid Pryadko, Chairperson
Dr. Michael Mulligan
Dr. Kirill Shtengel

The Dissertation of Michael Dean Woolls is approved:

Committee Chairperson

University of California, Riverside

Acknowledgments

I am grateful to my adviser, Dr. Pryadko, who has guided me since I was an undergrad. Nicolas Delfosse for a number of useful discussions. And my wife, who has supported me through this whole process.

This work was supported in part by the NSF Division of Physics via grants No. 1820939 and 1416578

ABSTRACT OF THE DISSERTATION

Percolation Transitions on Finite Transitive Hyperbolic Graphs

by

Michael Dean Woolls

Doctor of Philosophy, Graduate Program in Physics
University of California, Riverside, December 2020
Dr. Leonid Pryadko, Chairperson

Edge percolation on finite transitive graphs is studied analytically and numerically. The results are made rigorous by considering a sequence of finite graphs $(\mathcal{G}_t)_t$ covered by an infinite graph $\mathcal{H}$, and weakly convergent to $\mathcal{H}$. The covering maps are used to classify 1-cycles on graphs $\mathcal{G}_t$ as homologically trivial or nontrivial, and to define several thresholds associated with the rank of the first homology group on the open subgraphs. The growth of the homological distance d_t, the smallest size of a non-trivial cycle on $\mathcal{G}_t$, is identified as the main factor determining the location of homology changing thresholds. In particular, the giant cycle erasure threshold p_E^0 (related to the conventional erasure threshold for the corresponding sequence of generalized toric codes) coincides with the edge percolation threshold $p_c(\mathcal{H})$ if the ratio $d_t/\ln n_t$ diverges, where n_t is the number of edges of $\mathcal{G}_t$, and evidence is given that $p_E^0 < p_c(\mathcal{H})$ in several cases where this ratio remains bounded, which is necessarily the case if $\mathcal{H}$ is non-amenable.

Numerically, finite graphs are constructed with up to 10^5 edges from several families of locally-planar graphs covered by infinite transitive planar graphs parameterized by Schläfli symbols $\{f, d\}$ with $fd/(f + d) \geq 2$, where d regular f-gonal faces

meet in each vertex. Specifically, considered are the planar regular tiling $\{4,4\}$, regular hyperbolic tilings $\{3,7\}$, $\{3,8\}$, $\{4,5\}$, $\{4,6\}$, $\{5,5\}$, and $\{5,6\}$, their duals with f and d interchanged, as well as random graphs of degree $d = 5$—this latter family converges to an infinite tree of the same degree. Conventional and homological percolation are analyzed in these graphs, and the accuracy of several finite-size scaling methods designed calculate the cycle erasure threshold p_E^0, the conventional percolation threshold $p_c(\mathcal{H})$, and the giant cluster threshold p_G compared. In particular, the cluster ratio method, one of the most commonly used techniques to locate percolation thresholds, shows rather poor convergence for hyperbolic graphs of this type.

Contents

List of Figures

List of Tables

Chapter 1

Introduction

It is the threshold theorem [48, 52, 25, 17, 36, 33] that makes large-scale quantum computation feasible, at least in theory. Related is the notion of quantum channel capacity R_Q, such that for any rational $R < R_Q$, there exists a quantum error correcting code (QECC) with rate R which can be used to suppress the logical error probability to any chosen (arbitrarily small) level, but not for $R > R_Q$. Here the code rate $R \equiv k/n$ is the ratio of the number k of the logical (encoded) qubits to the length n of the code. The precise value of the capacity is not known for most quantum channels of interest, except for the *quantum erasure channel* with qubit erasure probability p, in which case $R_Q = \min(0, 1 - 2p)$, see Ref. [5].

In practice, it is often easier to deal with the threshold *error probability* for a given family (infinite sequence) of QECCs with certain asymptotic code rate R. Depending on the nature of the quantum channel in question, the threshold error probability may be related to the location of a thermodynamical phase transition in certain spin model associated with the codes. In particular, for a family of qubit toric codes on

transitive graphs locally isomorphic to a regular euclidean or hyperbolic tiling $\mathcal{H}$ under independent Z Pauli errors, the decoding threshold is upper bounded by the position of the multicritical point located at the Nishimori line of the Ising model on $\mathcal{H}$, see Refs. [17, 40, 32]. It is widely believed that the two thresholds coincide, at least for the euclidean tilings like the infinite square lattice and square-lattice toric codes. With a slightly more general model of independent X/Z Pauli errors, the threshold is the minimum of the corresponding thresholds for each error type which can be computed independently.

A special case is the relation between quantum erasure errors and percolation [14, 15, 16]. An erasure is formed by rendering inoperable all qubits in a known randomly selected set. Information loss happens when erasure covers a logical operator of the code. For certain code families, and for qubit erasure probability p sufficiently small, $p < p_E$, the probability to cover a codeword may go to zero as the code length n is increased to infinity. The corresponding threshold value p_E is called the *erasure threshold* associated with the chosen code family or code sequence. With a Calderbank-Shor-Steane (CSS) code [11, 51], one may consider the erasure thresholds for X and Z logical operators separately, so that the conventional erasure threshold becomes $p_E = \min(p_E^X, p_E^Z)$.

The link between erasure and percolation thresholds is especially simple in the case of toric/surface [35, 7, 22, 17, 13] and related quantum cycle codes [57] where qubits are labeled by the edges of a graph and, by convention, Z logical operators are supported on 1-chains in certain equivalence classes, e.g., those connecting two opposite boundaries of a rectangular region, or wrapped around a torus. Then, the erasure threshold p_E^Z

coincides with the discrete version of the homological percolation transition[6] for 1-chains. It is also known that for square-lattice toric code the erasure threshold p_E^Z coincides [50, 23] with the edge percolation threshold, $p_E^Z = p_c(\mathbb{Z}^2) = 1/2$. On the other hand, for a family of hyperbolic surface codes based on a given infinite graph $\mathcal{H}$, a regular tiling on the hyperbolic plane, we only know that the erasure threshold is upper bounded [14, 15, 16] by the percolation threshold on $\mathcal{H}$, $p_E \leq p_c(\mathcal{H})$.

Surely, the erasure and the percolation thresholds cannot always coincide. Indeed, percolation threshold is associated with the formation of an infinite cluster; it is defined on an infinite graph, while quantum codes are finite. Further, erasure threshold is not a bulk quantity, as it can be rendered zero by removing a vanishingly small fraction of well-selected qubits. Similarly, many different finite graphs can be associated with a given infinite graph $\mathcal{H}$, and it is not at all clear that the erasure threshold should remain the same independent of the details.

The goal of this work is to quantify the relation between edge percolation and the stability of quantum cycle codes (QCCs) to erasure errors. Specifically, we consider sequences of finite graphs $\mathcal{G}_t = (\mathcal{V}_t, \mathcal{E}_t)$, $t \in \mathbb{N}$, with a common infinite covering graph $\mathcal{H}$, and use the covering map $f_t : \mathcal{H} \to \mathcal{G}_t$ to identify homologically non-trivial cycles on $\mathcal{G}_t$. The distance $d_t \equiv d_{Z,t}$ of the corresponding quantum code (the smallest length of a non-trivial cycle) necessarily diverges with t when the sequence converges weakly to $\mathcal{H}$. First, we show that it is the scaling of d_t with the logarithm of the code block length, $n_t \equiv |\mathcal{E}_t|$, that determines the location of the Z-erasure threshold, or the 1-chain lower erasure threshold $p_E^Z \equiv p_E^0$, the point above which the probability of an open homologically non-trivial 1-cycle remains non-zero in the limit of arbitrarily large

graphs $\mathcal{G}_t$. Roughly, with sublogarithmic distance scaling, $d_t/\ln n_t \to 0$ as $t \to \infty$, $p_E^0 = 0$. On the other hand, with superlogarithmic distance scaling, $d_t/\ln n_t \to \infty$, p_E^0 coincides with the edge percolation threshold $p_{\mathrm{c}}(\mathcal{H})$, so that for $p < p_{\mathrm{c}}(\mathcal{H})$, probability to find an open homologically non-trivial 1-cycle be asymptotically zero. We also give an example of a graph family with logarithmic distance scaling, where the inequality in the upper bound is strict, $p_E^0 < p_{\mathrm{c}}(\mathcal{H})$, and give numerical evidence that for some regular tilings of the hyperbolic plane, erasure threshold is strictly below the percolation threshold, $p_E^0 < p_{\mathrm{c}}(\mathcal{H})$.

Second, the distance d_t grows at most logarithmically with n_t when $\mathcal{H}$ is non-amenable, which is also a necessary requirement to have a finite asymptotic code rate $k_t/n_t \to R > 0$, where k_t is the number of encoded qubits. For such a graph sequence, we define a pair of thermodynamical homological transitions, p_H^0 and p_H^1, which characterize singularities in the *erasure rate*, asymptotic ratio of the expected homology rank of the open subgraph and the number of edges n_t. Namely, erasure rate is zero for $p < p_H^0$, it saturates at R for $p > p_H^1$, and it takes intermediate values in the interval $p_H^0 < p < p_H^1$ (subsequence construction may be needed in this regime to achieve convergence). We prove that $p_H^1 - p_H^0 > R$, and, if $\mathcal{H}$ and its dual, $\widetilde{\mathcal{H}}$, is a pair of transitive planar graphs, we show that $p_H^0 = p_{\mathrm{c}}(\mathcal{H})$ and $p_H^1 = 1 - p_{\mathrm{c}}(\widetilde{\mathcal{H}})$; the latter point coincides with the uniqueness threshold $p_{\mathrm{u}}(\mathcal{H})$ on the original graph. We also conjecture that the two homological transitions coincide with the percolation and the uniqueness thresholds, respectively, for any non-amenable (quasi)transitive graph, $p_H^0 = p_{\mathrm{c}}(\mathcal{H})$ and $p_H^1 = p_{\mathrm{u}}(\mathcal{H})$.

In our numerical section we calculate three percolation thresholds: p_E^0, p_{c} and p_G. We compare our results with Ref. [45] and show their consistency with the

presented theorems. Mainly, we show $p_E^0 < p_c$ for hyperbolic graphs, and that the standard method which finds crossing point of the cluster ratio to calculate p_c [21] fails for hyperbolic graphs.

We find the percolation threshold on graphs whose cover is the $\{f, d\}$ tiling of the euclidean plane or hyper-plane. Mainly we use the following graphs types: $\{3, 7\}$, $\{7, 3\}$, $\{3, 8\}$, $\{8, 3\}$, $\{4, 5\}$, $\{5, 4\}$, $\{4, 6\}$, $\{6, 4\}$, $\{5, 5\}$, and $\{6, 5\}$, along with the planar $\{4, 4\}$ graph and a random graph with constant vertex degree of 5, $\{r, 5\}$.

The $\{r, 5\}$ and $\{4, 4\}$ graphs are included to show our numerical results are consistent with known exact results. Also, hyperbolic graphs are closely related to random graphs as they are both expander graphs and both have mean-field critical scaling, and so share many of the same properties. This allows us to relate results on the random graphs to hyperbolic graphs. However, we show that the cluster-ratio method used to calculate p_c works for random graphs, but not for the hyperbolic graphs.

The outline of this paper is as follows. In Sec. 2 we give the necessary notations. We present our analytical results in Sec. 3 and numerical results and methods in Sec. 4. In section 5 we give the conclusions and discuss some related open questions.

Chapter 2

Background

2.1 Classical binary and quantum CSS codes

A linear binary code with parameters $[n, k, d]$ is a vector space $\mathcal{C} \subseteq \mathbb{F}_2^n$ of length-n binary strings of dimension k, where the minimum distance d is the smallest Hamming weight of a non-zero vector in $\mathcal{C}$. Such a code $\mathcal{C} \equiv \mathcal{C}_G$ can be specified in terms of a generator matrix G whose rows are the basis vectors, or in terms of a parity check matrix H, $\mathcal{C} \equiv \mathcal{C}_H^\perp = \{c \in \mathbb{F}_2^n : Hc^T = 0\}$, where $\mathcal{C}_H^\perp$ denotes the space dual (orthogonal) to $\mathcal{C}_H$. A generator matrix and a parity check matrix of any length-n code satisfy

$$GH^T = 0, \quad \operatorname{rank} G + \operatorname{rank} H = n; \tag{2.1}$$

such matrices are called *mutually dual*.

If $I \subset \{1, \ldots, n\}$ is a set of bit indices, for any vector $b \in \mathbb{F}_2^n$, we denote $b[I]$ the corresponding *punctured* vector with positions outside of I dropped. Similarly, $G[I]$ (with columns outside of I dropped) generates the code $\mathcal{C}_G$ *punctured* to I, denoted $\mathcal{C}_G[I] \equiv \mathcal{C}_{G[I]}$. A *shortened* code is formed similarly, except by puncturing only the

vectors supported inside I,

$$\mathcal{C} \text{ shortened to } I = \{c[I] : \ c \in \mathcal{C} \ \wedge \ \mathrm{supp}(c) \subseteq I\}\,.$$

We use G_I to denote a generating matrix of the code $\mathcal{C}_G$ shortened to I. If G and H are a pair of mutually dual binary matrices, see Eq. (2.1), then H_I is a parity check matrix of the punctured code $\mathcal{C}_G[I]$ [41], and

$$\mathrm{rank}\, G[I] + \mathrm{rank}\, H_I = |I|, \tag{2.2}$$

i.e., matrices $G[I]$ and H_I are mutually dual. In addition, if $\overline{I} = \{1, 2, \ldots, n\} \setminus I$ is the complement of I, then

$$\mathrm{rank}\, G[\overline{I}] + \mathrm{rank}\, G_I = \mathrm{rank}\, G. \tag{2.3}$$

For the present purposes, it is sufficient that an n-qubit quantum CSS code $\mathcal{Q} = \mathrm{CSS}(G_X, G_Z)$ can be specified in terms of two n-column binary *stabilizer generator matrices* with mutually orthogonal rows, $G_X G_Z^T = 0$. It is isomorphic to a direct sum of two quotient spaces, $\mathcal{Q} = \mathcal{Q}_X \oplus \mathcal{Q}_Z$, where $\mathcal{Q}_X = \mathcal{C}_{G_Z}^{\perp}/\mathcal{C}_{G_X}$ and $\mathcal{Q}_Z = \mathcal{C}_{G_X}^{\perp}/\mathcal{C}_{G_Z}$. Vectors in $\mathcal{Q}_X$ and $\mathcal{Q}_Z$, respectively, are also called X- and Z-logical operators. Explicitly, $\mathcal{Q}_X$ is formed by vectors in $\mathcal{C}_{G_Z}^{\perp}$, with any two vectors that differ by an element of $\mathcal{C}_{G_X}$ identified (notice that $\mathcal{C}_{G_X} \subset \mathcal{C}_{G_Z}^{\perp}$). Such a pair of vectors $c' = c + \alpha G_X$ that differ by a linear combination of the rows of G_X are called mutually degenerate; we write $c' \simeq c$. The second half of the code, $\mathcal{Q}_Z$, is defined similarly, with the two generator matrices interchanged. For such Z-like vectors, the degeneracy is defined in terms of the rows of G_Z.

The distances d_X and d_Z of a CSS code are the minimum weights of non-trivial vectors in $\mathcal{Q}_X$ and $\mathcal{Q}_Z$, respectively, e.g., $d_X = \min\{\mathrm{wgt}\, c : c \in \mathcal{C}_{G_Z}^{\perp} \setminus \mathcal{C}_{G_X}\}$. Any

minimum-weight codeword is always *irreducible*, that is, it cannot be written as a sum of two vectors with disjoint supports, one of them being a codeword [19]. The conventional distance, the minimum weight of a logical operator in $\mathcal{Q}$, is $d = \min(d_X, d_Z)$. The dimension k of a CSS code is the dimension of the vector space $\mathcal{Q}_X$ (it is the same as the dimension of $\mathcal{Q}_Z$), the number of linearly independent and mutually non-degenerate vectors that can be used to form a basis of $\mathcal{Q}_X$. For a length-n code with stabilizer generator matrices G_X and G_Z,

$$k = n - \operatorname{rank} G_X - \operatorname{rank} G_Z. \tag{2.4}$$

The parameters of a quantum CSS code are commonly written as $[[n, k, (d_X, d_Z)]]$ or just $[[n, k, d]]$.

Any CSS code formed by matrices G_X and G_Z of respective dimensions $r_X \times n$ and $r_Z \times n$ also defines a binary chain complex with three non-trivial vector spaces,

$$\mathcal{A} : \ldots \leftarrow \{0\} \overset{\partial_0}{\leftarrow} \mathcal{A}_0 \overset{\partial_1}{\leftarrow} \mathcal{A}_1 \overset{\partial_2}{\leftarrow} \mathcal{A}_2 \overset{\partial_3}{\leftarrow} \{0\} \leftarrow \ldots, \tag{2.5}$$

where the spaces $\mathcal{A}_i = \mathbb{F}_2^{a_i}$ have dimensions $a_0 = r_X$, $a_1 = n$, and $a_2 = r_Z$, and the non-trivial boundary operators are expressed in terms of the generator matrices $\partial_1 = G_X$, $\partial_2 = G_Z^T$. This guarantees the defining property of a chain complex, $\partial_i \partial_{i+1} = 0$, $i \in \mathbb{Z}$. Then, the code $\mathcal{Q}_Z$ is defined identically to the first homology group $H_1(\mathcal{A}) = \ker(\partial_1)/\operatorname{im}(\partial_2)$, where elements of $\operatorname{im}(\partial_2)$ called *cycles* are linear combinations of the columns of $\partial_2 = G_Z^T$, while elements of $\ker(\partial_1)$ called *boundaries* are vectors orthogonal to the rows of $\partial_1 = G_X$. The other definitions also match. In particular, the dimension k of the quantum code is the rank of the first homology group, $k = \operatorname{rank} H_1(\mathcal{A})$, while the definition of the homological distance $d_1(\mathcal{A})$ matches that of d_Z. The other code,

$\mathcal{Q}_X$, corresponds to the co-homology group defined in the co-chain complex $\widetilde{\mathcal{A}}$ formed similarly but with the two matrices interchanged.

Let us now consider the structure of the homology group where the space $\mathcal{A}_1$ is restricted so that only components with indices in the index set $I \subset \{1, 2, \ldots, n\}$ be non-zero. Respectively, the spaces $\ker \partial_1 = \mathcal{C}_{G_X}^{\perp}$ and $\operatorname{im} \partial_2 = \mathcal{C}_{G_Z}$ should be replaced with the corresponding reduced spaces. The result is isomorphic to a chain complex $\mathcal{A}'_I$ where the two boundary operators are obtained by puncturing and shortening, respectively: $\partial'_1 = G_X[I]$ and $\partial'_2 = (G_Z)_I^T$. The dimension of thus defined restricted homology group is given by

$$k'_I \equiv \operatorname{rank} H_1(\mathcal{A}'_I) = |I| - \operatorname{rank} G_X[I] - \operatorname{rank}(G_Z)_I. \tag{2.6}$$

Using Eq. (2.3), we also get [15]

$$k'_I = |I| - \operatorname{rank} G_Z - \operatorname{rank} G_X[I] + \operatorname{rank} G_Z[\overline{I}]. \tag{2.7}$$

The corresponding result for the rank $\tilde{k}'_I$ of the restricted co-homology group can be found by exchanging the matrices G_X and G_Z; this gives the duality relation

$$k'_I + \tilde{k}'_{\overline{I}} = k. \tag{2.8}$$

2.2 Graphs, cycles, and cycle codes

We consider only simple graphs with no loops or multiple edges. A graph $\mathcal{G} = (\mathcal{V}, \mathcal{E})$ is specified by its sets of vertices $\mathcal{V} \equiv \mathcal{V}_\mathcal{G}$, also called sites, and edges $\mathcal{E} \equiv \mathcal{E}_\mathcal{G}$. Each edge $e \in \mathcal{E}$ is a set of two vertices, $e = \{u, v\}$; it can also be denoted with a wave, $u \sim v$. For every vertex $v \in \mathcal{V}$, its degree $\deg(v)$ is the number of edges that include v. An infinite graph $\mathcal{G}$ is called quasi-transitive if there is a finite subset $\mathcal{V}_0 \subset \mathcal{V}_\mathcal{G}$ of its

vertices, such that for every vertex $v \in \mathcal{V}$ there is an automorphism (symmetry) of $\mathcal{G}$ mapping v to an element of $\mathcal{V}_0$. A transitive graph is a quasi-transitive graph where the subset $\mathcal{V}_0$ of vertex classes contains only one element. All vertices in a transitive graph have the same degree.

We say that vertices u and v are connected on $\mathcal{G}$ if there is a path $P \equiv P(u_0, u_\ell)$ between $u \equiv u_0$ and $v \equiv u_\ell$, a set of edges which can be ordered and oriented to form a *walk*, a sequence of vertices starting with u and ending with v, with each directed edge in P matching the corresponding pair of neighboring vertices in the sequence,

$$P(u_0, u_\ell) = \{u_0 \sim u_1, u_1 \sim u_2, \ldots, u_{\ell-1} \sim u_\ell\} \subseteq \mathcal{E}. \tag{2.9}$$

We call such a path open if $u_0 \neq u_\ell$, and closed otherwise. The path is called self-avoiding (simple) if $u_i \neq u_j$ for any $0 \leq i < j \leq \ell$, except that u_0 and u_ℓ coincide if the path is closed. The length of the path is the number of edges in the set, $\ell = |P|$. The distance $d(u, v)$ between vertices u and v is the smallest length of a path between them. Given a vertex $v \in \mathcal{V}$ and a natural $r \in \mathbb{N}$, a ball $\mathcal{B}(v, r; \mathcal{G})$ is the subgraph of $\mathcal{G}$ induced by the vertices $u \in \mathcal{V}$ such that $d(v, u) \leq r$.

The edge boundary $\partial\mathcal{U}$ of a set of vertices $\mathcal{U} \subseteq \mathcal{V}$ is the set of edges connecting $\mathcal{U}$ and its complement $\overline{\mathcal{U}} \equiv \mathcal{V} \setminus \mathcal{U}$. Given an exponent $\alpha \leq 1$, we define the isoperimetric constant of a graph,

$$b_\alpha = \inf_{\emptyset \neq \mathcal{U} \subsetneq \mathcal{V}, |\mathcal{U}| \neq \infty} \frac{|\partial\mathcal{U}|}{\left[\min\left(|\mathcal{U}|, |\overline{\mathcal{U}}|\right)\right]^\alpha}. \tag{2.10}$$

For an infinite graph, or a set of finite graphs that includes graphs of arbitrarily large size, particularly important is the largest α such that the corresponding $b_\alpha > 0$. Such a graph (or graph family) is called an α-expander; when $\alpha < 1$, the related parameter $\delta \equiv (1 - \alpha)^{-1}$ is called the isoperimetric dimension. Isoperimetric dimension of any

regular D-dimensional lattice is $\delta = D$. When $\alpha = 1$, the isoperimetric constant b_1 of a graph $\mathcal{G}$ is called its Cheeger constant, $h(\mathcal{G}) = b_1$. An infinite graph with a non-zero Cheeger constant is called non-amenable.

A set of edges $C \subseteq \mathcal{E}$ is called a cycle if the degree of each vertex in the subgraph induced by C, $\mathcal{G}' = (\mathcal{V}, C)$, is even. The set of all cycles on a graph $\mathcal{G}$, with the symmetric difference defined as $A \oplus B \equiv (A \backslash B) \cup (B \backslash A)$ used as the group operation, forms an abelian group, the *cycle group* of $\mathcal{G}$, denoted $\mathcal{C}(\mathcal{G})$. Clearly, a closed path is a cycle. A simple cycle is a self-avoiding closed path.

A graph $\mathcal{H}$ is called a covering graph of $\mathcal{G}$ if there is a function f mapping $\mathcal{V}_\mathcal{H}$ onto $\mathcal{V}_\mathcal{G}$, such that an edge $(u, v) \in \mathcal{E}_\mathcal{H}$ is mapped to the edge $\big(f(u), f(v)\big) \in \mathcal{E}_\mathcal{G}$, with an additional property that f be invertible in the vicinity of each vertex, i.e., for a given vertex $u' \in \mathcal{V}_\mathcal{H}$ and an edge $(f(u'), v) \in \mathcal{E}_\mathcal{G}$, there must be a unique edge $(u', v') \in \mathcal{E}_\mathcal{H}$ such that $f(v') = v$. As a result, given a path P connecting vertices u and v on $\mathcal{G}$ and a vertex $u' \in \mathcal{V}_\mathcal{H}$ such that $f(u') = u$, there is a unique path P' on $\mathcal{H}$, the lift of P, such that f maps the sequence of vertices $u'_0 \equiv u$, u'_1, u'_2, ... in P' to that in P. To simplify the notations, we will in some cases write a covering map as a map between the graphs, $f : \mathcal{H} \to \mathcal{G}$.

A set of vertices u' with the same covering map image u, $f(u') = u$, is called the *fiber* of u. A lift of a closed path starting and ending with u is either a closed path, or an open path connecting two different vertices in the fiber of u. We call a simple cycle on $\mathcal{G}$ homologically trivial if all its lifts are simple cycles (of the same length). A cycle on $\mathcal{G}$ is trivial if it is a union of edge-disjoint homologically trivial simple cycles. The set of trivial cycles on $\mathcal{G}$, with "$\oplus$" used for group operation, is a subgroup of

the cycle group on $\mathcal{G}$. We denote such a group $\mathcal{C}_0(\mathcal{H}; f)$. The corresponding group quotient, $H_1(f) \equiv \mathcal{C}(\mathcal{G})/\mathcal{C}_0(\mathcal{H}; f)$, is the (first) homology group associated with the map f; its elements are equivalence classes formed by sets of cycles whose elements differ by an addition of a trivial cycle. Namely, cycles C and C' are equivalent, $C' \simeq C$, if $C' = C \oplus C_0$, with $C_0 \in \mathcal{C}_0(\mathcal{H}; f)$.

The cycle space of a graph $\mathcal{G} = (\mathcal{V}, \mathcal{E})$ with $n = |\mathcal{E}|$ edges can be defined algebraically in terms of the vertex-edge incidence matrix $J \equiv J_{\mathcal{G}}$. Namely, it is isomorphic to the binary code $\mathcal{C}_J^{\perp} \subset \mathbb{F}_2^n$ whose parity check matrix is the incidence matrix J, $\mathcal{C}(\mathcal{G}) \cong \mathcal{C}_J^{\perp}$. On the other hand, the code $\mathcal{C}_J$ generated by the incidence matrix is isomorphic to the cut space of the graph. Elements of the cut space are edge boundaries $\partial\mathcal{U}$ of different partitions defined by sets of vertices $\mathcal{U} \subset \mathcal{V}$.

In principle, any set $\mathcal{C}' \subset \mathcal{C}(\mathcal{G})$ of cycles on $\mathcal{G}$ can be used to construct a binary matrix K with the rows orthogonal to J, $JK^T = 0$; the code $\mathcal{C}_K \subset \mathbb{F}_2^n$ is isomorphic to the subspace of the cycle space generated by elements of $\mathcal{C}'$. In particular, given the covering map $f : \mathcal{H} \to \mathcal{G}$, such a matrix K can be constructed using a basis set of homologically trivial cycles $\mathcal{C}_0(\mathcal{H}; f)$. Thus, such a covering map has a chain complex (2.5) associated with it, where $\mathcal{A}_0$, $\mathcal{A}_1$, and $\mathcal{A}_2$ are spaces generated by sets of vertices, edges, and homologically trivial cycles, respectively. In particular, the support $\mathrm{supp}(a)$ of any vector $a \in \mathcal{A}_1$ corresponds to a set of edges. The boundary operators are given by the constructed matrices $\partial_1 = J$, $\partial_2 = K^T$. Equivalently, the same matrices can be used to define a stabilizer code $\mathrm{CSS}(J, K)$ with generators $G_X = J$ and $G_Z = K$. We will denote such a *quantum cycle code* associated with the covering map $f : \mathcal{H} \to \mathcal{G}$ as $\mathcal{Q}(\mathcal{H}; f)$. The length of the code is $n = |\mathcal{E}|$, the number of encoded

qubits $k = \operatorname{rank} H_1(\mathcal{A})$ is the rank of the first homology group associated with covering map, and the distances d_Z, d_X, respectively, are the homological distances $d_1(\mathcal{A})$, $d_1(\widetilde{\mathcal{A}})$ associated with the chain complex $\mathcal{A}$ and the co-chain complex $\widetilde{\mathcal{A}}$.

Given a graph $\mathcal{H} = (\mathcal{V}, \mathcal{E})$ and a subgroup Γ of its automorphism group $\mathrm{Aut}(\mathcal{H})$, consider the partition of $\mathcal{V}$ induced by Γ, where a pair of vertices u, v are in the same class iff there is an element $g \in \Gamma$ such that $g(u) = v$. Then, the *quotient graph* $\mathcal{G} = \mathcal{H}/\Gamma$ has the vertex set given by the set of vertex classes, with an edge between any two classes which contain a pair of vertices connected by an edge from $\mathcal{E}$. A graph quotient $\mathcal{H}/\Gamma$ is covered by $\mathcal{H}$ if no neighboring vertices fall into the same class. When $\mathcal{H}$ is infinite, a finite quotient graph $\mathcal{H}/\Gamma$ is obtained if the subgroup Γ has a finite index; in such a case $\mathcal{H}$ must be quasitransitive.

A graph, $\mathcal{G}$, has a dual graph, $\widetilde{\mathcal{G}}$, iff it is locally planar. A locally planar graph is any graph which can be embedded onto a two dimensional simple manifold. If the manifold is the plane, then $\mathcal{G}$ is called planar. The trivial cycle space of locally planar graph $\mathcal{G}$, $\mathcal{C}_0$, is called the *face space* of $\mathcal{G}$. If $\mathcal{G}$ is locally planar then all edges of $\mathcal{G}$ are incident to exactly 2 basis cycles of $\mathcal{C}_0$. This allows us to define a dual graph.

Dual graphs $\mathcal{G}$ and $\widetilde{\mathcal{G}}$ have equivalent edge spaces, $\mathcal{E} = \widetilde{\mathcal{E}}$, such that each edge in $\mathcal{E}$ has a corresponding dual edge in $\widetilde{\mathcal{E}}$. If $\mathcal{H}$ is the cover of $\mathcal{G}$, and $\widetilde{\mathcal{H}}$ is the dual of $\mathcal{H}$, then the image of $\widetilde{\mathcal{H}}$, with the same covering map, is the graph $\widetilde{\mathcal{G}}$, the dual of $\mathcal{G}$, and dual edges between $\mathcal{H}$ and $\widetilde{\mathcal{H}}$ map to dual edges on $\mathcal{G}$ and $\widetilde{\mathcal{G}}$. Also, the cycle space of $\mathcal{H}$ is equivalent to the cut space of $\widetilde{\mathcal{H}}$,

$$\mathcal{C}(\mathcal{H}) = \mathcal{C}^{\perp}(\widetilde{\mathcal{H}}). \tag{2.11}$$

2.3 Percolation transitions

We only consider Bernoulli edge percolation, where each edge $e \in \mathcal{E}$ of a graph $\mathcal{H} = (\mathcal{V}, \mathcal{E})$ is independently labeled as open or closed, with probabilities p and $1 - p$, respectively. We are focusing on the subgraph $[\mathcal{G}]_p$ remaining after removal of all closed edges; connected components of $[\mathcal{G}]_p$ are called clusters. For a given $v \in \mathcal{V}$, the cluster which contains v is denoted $\mathcal{K}_v \subseteq [\mathcal{G}]_p$. If $\mathcal{K}_v$ is infinite, for some v, we say that percolation occurs.

If two graphs, $\mathcal{G}$ and $\widetilde{\mathcal{G}}$, are mutually dual we can perform edge percolation on both graphs at once, such that when an edge is open on $\mathcal{G}$ then it is closed on $\widetilde{\mathcal{G}}$ and vice-versa. Fig. 2.1 shows a small example of this. Picking some p value and generating the corresponding subgraphs $[\mathcal{G}]_p$ and $[\widetilde{\mathcal{G}}]_p$ we have Euler's formula on each subgraph,

$$\operatorname{rank} \mathcal{C} = n - |\mathcal{V}| + k, \tag{2.12}$$

where k is the number of connected components, or clusters. The dual of each trivial cycle on $\mathcal{G}$ is a cut on $\widetilde{\mathcal{G}}$, due to equation 2.11. Therefore, for each cluster on $[\widetilde{\mathcal{G}}]_p$ their is an open trivial cycle on $[\mathcal{G}]_p$, and knowing there must always be at least one cluster, we deduce

$$\operatorname{rank} \mathcal{C}_0 = \widetilde{k} - 1, \tag{2.13}$$

where $\widetilde{k}$ is the number of clusters on $[\widetilde{\mathcal{G}}]_p$. If we combine equations 2.13 and 2.12 we conclude

$$\operatorname{rank} H_1 = k - \widetilde{k} + n - |\mathcal{V}| + 1, \tag{2.14}$$

where we have used the fact

$$\operatorname{rank} \mathcal{C} = \operatorname{rank} \mathcal{C}_0 + \operatorname{rank} H_1. \tag{2.15}$$

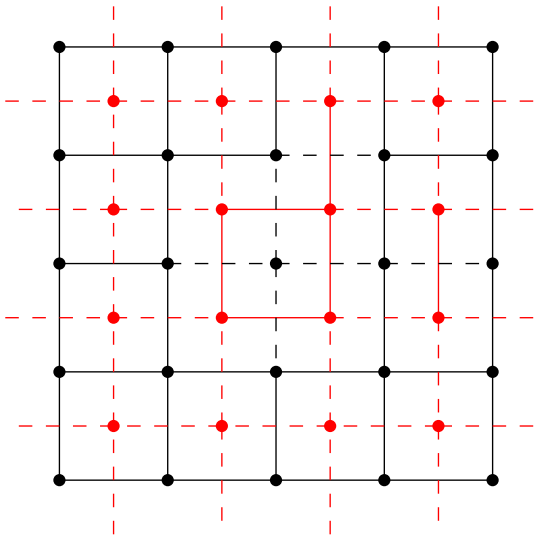

Figure 2.1: An example of two dual graphs, one black and the other red. The dashed lines are closed edges, while the solid lines are open edges. Each red edge with only one connected end all meet up at a single vertex not shown. Note: the red graph has 11 clusters and 1 cycle and the black graph has 2 clusters and 10 cycles which agrees with equation 2.13.

Three observables are usually associated with percolation: the probability that vertex v is in an infinite cluster,

$$\theta_v \equiv \theta_v(\mathcal{H}, p) = \mathbb{P}_p(|\mathcal{K}_v| = \infty), \tag{2.16}$$

the connectivity function,

$$\tau_{u,v} \equiv \tau_{u,v}(\mathcal{H}, p) = \mathbb{P}_p\big(u \in \mathcal{K}_v\big), \tag{2.17}$$

the probability that vertices u and v are in the same cluster, and the local cluster susceptibility,

$$\chi_v \equiv \chi_v(\mathcal{H}, p) = \mathbb{E}_p(|\mathcal{K}_v|), \tag{2.18}$$

the expected size of the cluster connected to v. Equivalently, cluster susceptibility can be defined as the sum of probabilities for individual vertices to be in the same cluster

as v, i.e., as a sum of connectivities,

$$\chi_v = \sum_{u \in \mathcal{V}} \tau_{v,u}. \tag{2.19}$$

The critical propability p_c, the percolation threshold, is associated with the formation of an infinite cluster, defined as

$$p_c = \inf\{p : \theta(p) > 0\}. \tag{2.20}$$

So, there is no percolation, $\theta_v = 0$, for $p < p_c$, but $\theta_v > 0$ for $p > p_c$. An equivalent definition is based on the existence of an infinite cluster anywhere on $[\mathcal{H}]_p$; the probability of finding such a cluster is zero at $p < p_c$, and one at $p > p_c$, see, e.g., Theorem (1.11) in Ref. [26] (the same proof works for any infinite connected graph).

Similarly, the critical probability p_T is associated with divergence of site susceptibilities: χ_v is finite for $p < p_T$ but not for $p > p_T$. Again, in a connected graph, this definition does not depend on the choice of $v \in \mathcal{V}$. If percolation occurs (i.e., with probability $\theta_v > 0$, $|\mathcal{K}_v| = \infty$), then clearly $\chi_v = \infty$. This implies $p_c \geq p_T$. The reverse is known to be true for percolation on quasi-transitive graphs [43, 44]: $\chi_v = \infty$ can only happen inside or on the boundary of the percolation phase. Thus, for a quasi-transitive graph, $p_c = p_T$.

An important question is the number of infinite clusters on $[\mathcal{H}]_p$, in particular, whether an infinite cluster is unique. For infinite quasi-transitive graphs, there are only three possibilities: (**a**) almost surely there are no infinite clusters; (**b**) there are infinitely many infinite clusters; and (**c**) there is only one infinite cluster [4, 27, 55]. A third critical probability, p_u, is associated with the number of infinite clusters. Most generally, we

expect $p_T \leq p_c \leq p_u$. For a quasi-transitive graph, one has [55]

$$0 < p_T = p_c \leq p_u. \tag{2.21}$$

Here, p_u is the uniqueness threshold, such that there can be only one infinite cluster for $p > p_u$, whereas for $p < p_u$, the number of infinite clusters may be zero, or infinite. For an amenable quasitransitive graph, $p_c = p_u$ [1, 10, 34]; it was conjectured by Benjamini and Schramm[4] that $p_c < p_u$ for non-amenable quasi-transitive graphs. Among other examples, the conjecture has been recently verified for a large class of Gromov-hyperbolic graphs[31].

In order for the uniqueness threshold to be non-trivial, $p_u < 1$, the graph $\mathcal{H}$ has to have only one end. That is, it can not be separated into two or more infinite components by removing a finite number of edges.

In addition to uniqueness of the infinite cluster, the same threshold p_u can be characterized in terms of the connectivity function [54]. Namely, $\inf_{u,v\in\mathcal{V}} \tau_{u,v}(p) > 0$ for $p > p_u$ and it is zero for $p < p_u$. Further, for planar transitive graphs, the uniqueness threshold is related to the percolation threshold on the dual graph,

$$p_u(\mathcal{H}) = 1 - p_c(\widetilde{\mathcal{H}}), \tag{2.22}$$

see the proof of Theorem 7.1 in Ref. [27]. In the case of planar amenable graphs where $p_c(\mathcal{H}) = p_u(\mathcal{H})$, the duality (2.22) is between the two percolation transitions [26].

For finite size graphs the giant cluster threshold, p_G, is commonly used instead of p_c. For $p > p_G$ the largest sized cluster scales proportional to the size of the graph, while for $p < p_G$ it does not. More precisely, given a finite graph sequence, $(\mathcal{G}_t)_t$, with cover $\mathcal{H}$, the covering map f_t and injectivity radius r_t, let $s_1(p;\mathcal{G}_t) = S_1(p;\mathcal{G}_t)/|\mathcal{V}_t|$ be

the fractional size of the largest cluster. Then we define p_G to be

$$p_G = \inf_{p>0}\{p : \limsup_{t\to\infty} s_1(p;\mathcal{G}_t) > 0\}. \tag{2.23}$$

It is easy to see that in general $p_G \geq p_{\mathrm{c}}(\mathcal{H})$. Moreover, on expander graphs, we have $p_G = p_c$ [Theorem 1.3 in [3]]. A similar statement is also true for a torus in $\mathbb{Z}^D$.

Chapter 3

Homology-Changing Transitions

Consider a finite graph $\mathcal{G} = (\mathcal{V}_\mathcal{G}, \mathcal{E}_\mathcal{G})$ covered by an infinite graph $\mathcal{H} = (\mathcal{V}, \mathcal{E})$. While the graph $\mathcal{H}$ need not be quasi-transitive, the set of vertex degrees of $\mathcal{H}$ is finite and matches that of $\mathcal{G}$; in particular, the two graphs have the same maximal degree $\Delta_{\max}$. The covering map $f : \mathcal{V} \to \mathcal{V}_\mathcal{G}$ also defines a quantum cycle code $\mathcal{Q}(\mathcal{H}; f)$ with parameters $[[n, k, (d_X, d_Z)]]$, where $n = |\mathcal{E}_\mathcal{G}|$ the number of edges in $\mathcal{G}$, and $k = \operatorname{rank} H_1(f)$ the dimension of the first homology group associated with the map f. We are particularly interested in the case where the graphs $\mathcal{G}$ and $\mathcal{H}$ look identical on some scale. Formally, this is formulated in terms of the injectivity radius, defined as the largest integer r_f such that the map f is one-to-one in any ball $\mathcal{B}(v, r_f; \mathcal{H})$. Necessarily, for any covering map f, the injectivity radius $r_f \geq 1$. We start by giving lower bounds for the distances d_X, d_Z in terms of the injectivity radius.

First, an injectivity radius r_f implies that no two vertices located at distance r_f or smaller from any vertex on $\mathcal{H}$ map to the same vertex on $\mathcal{G}$. On the other hand, any simple cycle $C \subset \mathcal{G}$ of length ℓ is for sure covered by a ball of radius $r = \lceil \ell/2 \rceil$

centered on a vertex in C. This gives:

Lemma 1 *Consider a finite graph $\mathcal{G}$ covered by an infinite graph $\mathcal{H}$, with the injectivity radius r_f. Then the minimum weight d_Z of a non-trivial cycle on $\mathcal{G}$ satisfies the inequality $2r_f + 1 \leq d_Z \leq 2r_f + 3$.*

Proof. Let $C \subset \mathcal{E}_\mathcal{G}$ be a non-trivial cycle of weight d_Z, and $v \in \mathcal{V}_\mathcal{G}$ a vertex on C. Let $v' \in \mathcal{V}$ be a vertex from the fiber of v, then the ball $\mathcal{B} \equiv \mathcal{B}(v', r_f; \mathcal{H})$ is mapped one-to-one by f. Since $\mathcal{C}$ is non-trivial, it must contain at least one edge outside of the image of $\mathcal{B}$. Since $\mathcal{C}$ is also a minimum-weight non-trivial cycle, it must be self-avoiding, i.e., it should contain two edge-disjoint paths connecting v to the boundary of the image of $\mathcal{B}$. Necessarily, $d_Z > 2r_f$.

Conversely, consider a ball $\mathcal{B}_1$ of radius $r_f + 1$ which covers a non-trivial cycle C_1 on $\mathcal{G}$ of weight w, the shortest cycle among those covered by $\mathcal{B}_1$. At most two vertices of C_1 are at the distance $r_f + 1$ from u (otherwise a shorter cycle could be constructed), which gives $d_Z \leq w \leq 2r_f + 3$. ■

Second, the minimum distance d_X is the minimum size of a homologically non-trivial *co-cycle*, a set of edges on $\mathcal{G}$ which has even overlap with any homologically trivial cycle, but is not a cut of $\mathcal{G}$. A lower bound for d_X requires some additional assumptions:

Lemma 2 *Consider a finite graph $\mathcal{G}$ covered by an infinite one-ended graph $\mathcal{H}$, with the injectivity radius r_f. Assume that the cycle group of $\mathcal{H}$ can be generated by cycles of weight not exceeding $\omega \geq 3$. Then, the minimum weight of a non-trivial co-cycle on $\mathcal{G}$ satisfies the inequality $d_X > r_f/\omega$.*

Proof. The statement is trivial if $r_f < \omega$, since $d_X \geq 1$ by definition. Assume

$r_f \geq \omega$, so that any generator of the cycle group on $\mathcal{H}$ be mapped one-to-one. Thus, any (finite) cycle on $\mathcal{H}$ is mapped to a homologically trivial cycle, where we assume that the symmetric set difference "$\oplus$" be used when an edge is encountered in the image more than once. Consequently, a lift of a walk cycling around a simple non-trivial cycle C on $\mathcal{G}$ cannot be closed; instead, it must be a portion of a semi-infinite self-avoiding path on $\mathcal{H}$. Respectively, for any edge $e_0 \in C$ and its lift $e'_0 \in \mathcal{E}$ such that $f(e'_0) = e_0$, we denote $C' \equiv C'(C, e'_0) \ni e'_0$, the *extended lift* of C, the union of lifts of all walks on C starting with e'_0 and e_0, respectively; C' is an infinite self-avoiding path.

Now, take a binary vector b with $\mathrm{wgt}(b) = d_X$ such that $B \equiv \mathrm{supp}(b) \subset \mathcal{E}_\mathcal{G}$ be a minimum-weight non-trivial co-cycle on $\mathcal{G}$. Then, it must be irreducible, which implies that B must be *cycle-connected*, i.e., for any pair of edges $e_\mathrm{i} \neq e_\mathrm{f}$ in B, it should also contain a connecting edge sequence $\mathcal{S} = (e_1 = e_\mathrm{i}, e_2, \ldots, e_{m-1}, e_m = e_\mathrm{f}) \subseteq B$, with any pair of neighboring edges sharing an image of a basis cycle on $\mathcal{H}$. Given such a sequence of length m, the conventional graph distance between any pair of vertices from the union $e_\mathrm{i} \cup e_\mathrm{f}$ must be strictly smaller than ωm.

To prove the contrary, let us assume that $d_X \leq r_f/\omega$. Then, a minimum-weight co-cycle $B \subset \mathcal{E}_\mathcal{G}$ must have a diameter strictly smaller than r_f, i.e., there be a ball $\mathcal{B}_r \subset \mathcal{G}$ of radius $r \leq r_f$ such that $B \subset \mathcal{B}_r$. Indeed, with $\mathrm{wgt}(B) = d_X$, any connecting sequence contains at most $m = d_X$ edges, which implies the conventional distance between any pair of vertices on B smaller than $d_X\omega \leq r_f$. This implies that any lift B' of B should be mapped one-to-one by f.

To finish the proof, let $C \subset \mathcal{E}_\mathcal{G}$ be an irreducible cycle conjugate to B, i.e., the corresponding binary vectors satisfy $bc^T = 1$, which implies the existence of an edge

$e_0 \in B \cap C$. Irreducibility of C implies that it must be a simple cycle on $\mathcal{G}$. Given e_0' such that $f(e_0') = e_0$, let $B' \ni e_0'$ be a lift of B and $C' = C'(C, e_0')$ an extended lift of C, an infinite self-avoiding path on $\mathcal{H}$. Since B' is mapped one-to-one by f, it has odd-weigh intersection with C' and even-weight intersection with any basis cycle on $\mathcal{H}$. Respectively, B' must have an odd-weight intersection with any deformation $\bar{C}' \equiv C' \oplus M$ of C', where $M \subset \mathcal{C}_H$ is a finite cycle on H. Thus, B' is a finite-size cut splitting $\mathcal{H}$ into infinite portions, which can not be the case since $\mathcal{H}$ is assumed one-ended. ■

In addition, it will be important that for any covering map $f : \mathcal{H} \to \mathcal{G}$, the vertices of $\mathcal{G}$ can be lifted in such a way that they induce a connected subgraph of $\mathcal{H}$, just as a square-lattice torus with periodic boundary conditions becomes a rectangular piece of the square lattice after cutting two rows of edges.

Lemma 3 *Let $\mathcal{G}$ be a finite connected graph, $\mathcal{H}$ its cover with the covering map $f : \mathcal{V} \to \mathcal{V}_\mathcal{G}$ and the injectivity radius r_f. For any $v' \in \mathcal{V}$ let $v \equiv f(v') \in \mathcal{V}_\mathcal{G}$ be its image. Then there exists a set of vertices $\mathcal{V}_f \subset \mathcal{V}$ which contains a unique representative from the fiber of every vertex of $\mathcal{V}_\mathcal{G}$, such that the subgraph $\mathcal{H}_f \subset \mathcal{H}$ induced by $\mathcal{V}_f$ be connected and contains the ball $\mathcal{B}(v', r_f; \mathcal{H})$.*

Proof. Consider a graph $\mathcal{G}'$ obtained from $\mathcal{G}$ by removing the ball $\mathcal{B} \equiv \mathcal{B}(v, r_f; \mathcal{G})$. Construct a connected graph $\mathcal{G}''$ from a union of $\mathcal{B}$ and spanning trees of every connected component of $\mathcal{G}'$, by sequentially adding bridge bonds connecting individual components so that no new cycles are introduced. Such a subgraph contains all vertices of $\mathcal{G}$ and can be lifted to $\mathcal{H}$ starting with v'; let $\mathcal{V}_f \subset \mathcal{V}_\mathcal{H}$ be the corresponding vertex set. By construction, f acts one-to-one on $\mathcal{V}_f$. It is also easy to check that $\mathcal{H}_f$,

the subgraph of $\mathcal{H}$ induced by $\mathcal{V}_f$, be connected. ■

In the following, we consider not a single graph $\mathcal{G}$, but a sequence $(\mathcal{G}_t)_{t\in\mathbb{N}}$ of finite graphs $\mathcal{G}_t = (\mathcal{V}_t, \mathcal{E}_t)$ sharing an infinite connected covering graph $\mathcal{H} = (\mathcal{V}, \mathcal{E})$, with the covering maps $f_t : \mathcal{V} \to \mathcal{V}_t$. If the corresponding sequence of injectivity radii $r_t \equiv r_{f_t}$ diverges, we say that the sequence $(\mathcal{G}_t)_t$ weakly converges to $\mathcal{H}$. Such a convergent sequence can be constructed, e.g., as a sequence of finite quotients of the graph $\mathcal{H}$ with respect to a sequence of subgroups of its symmetry group, which requires $\mathcal{H}$ to be quasitransitive. We do not know whether quasitransitivity of $\mathcal{H}$ is necessary to have a sequence of finite graphs covered by $\mathcal{H}$ and weakly convergent to $\mathcal{H}$. By this reason, in the following, we specify (quasi)transitivity only when necessary for the corresponding proof.

Given a graph sequence with a common covering graph $\mathcal{H}$, we use $\mathcal{Q}_t$ to denote the CSS code with parameters $[[n_t, k_t, (d_{Xt}, d_{Zt})]]$ associated with the covering map f_t. We also denote the "flattened" subgraphs from Lemma 3 as $\mathcal{H}_t \equiv \mathcal{H}_{f_t} \subset \mathcal{H}$. When the sequence $(r_t)_t$ diverges, we can always construct a subsequence $(t_s)_s$, $t_{s+1} > t_s$, such that the corresponding sequence of graphs $(\mathcal{H}_{t_s})_s$ be increasing, $\mathcal{H}_{t_{s+1}} \subsetneq \mathcal{H}_{t_s}$. To this end, it is sufficient to take $r_{t_{s+1}} > n_{t_s}$, regardless of the particular spanning trees used in the construction of the graphs $\mathcal{H}_t$.

3.1 Homology erasure thresholds

Coming back to percolation, let $H_1(f_t, p)$ denote the first homology group formed by classes of homologically non-trivial cycles on the open subgraph $[\mathcal{G}_t]_p$. We will consider several observables that quantify the changes in homology in the open

subgraphs at large t as the probability p is increased. The first two, defined by analogy with corresponding quantities for 1-cycle proliferation in continuum percolation [6], are designed to detect any changes in homology compared to the empty graphs at $p = 0$, and the graphs with all edges present at $p = 1$. Respectively, we define the probability that a homologically non-trivial cycle exists in the open subgraph,

$$\mathbf{P}_E(t,p) \equiv \mathbb{P}_p\big(\operatorname{rank} H_1(f_t,p) \neq 0\big), \tag{3.1}$$

and the probability that not all homologically non-trivial cycles are covered in the open subgraph,

$$\mathbf{P}_A(t,p) \equiv \mathbb{P}_p\big(\operatorname{rank} H_1(f_t,p) \neq k_t\big). \tag{3.2}$$

Equivalently, $\mathbf{P}_A(t,p)$ is the probability that the open subgraph at $\bar{p} = 1-p$ covers a homologically non-trivial co-cycle. In terms of the associated CSS code $\mathcal{Q}_t$, $\mathbf{P}_E(t,p)$ and $\mathbf{P}_A(t,1-p)$ are the erasure probabilities for a Z- and an X-type codeword, respectively. These quantities do not necessarily characterize bulk phase(s), as they may be sensitive to the state of a sublinear number of edges.

As p is increasing from 0 to 1, $\mathbf{P}_E(t,p)$ is monotonously increasing from 0 to 1 while $\mathbf{P}_A(t,p)$ is monotonously decreasing from 1 to 0. Thus, a version of the subsequence construction can be used to ensure the existence of their $t \to \infty$ limits almost everywhere on the interval $p \in [0,1]$. Instead, we define the (lower) cycle erasure threshold for any given graph sequence,

$$p_E^0 = \sup\left\{p \in [0,1] : \lim_{t\to\infty} \mathbf{P}_E(t,p) = 0\right\}. \tag{3.3}$$

Because of monotonicity of $\mathbf{P}_E(t,p)$ as a function of p, a zero limit at some $p = p_0 > 0$ ensures the limit exists and remains the same everywhere on the interval $p \in [0,p_0]$.

Further, the absence of convergence of the sequence $\mathbf{P}_E(t,p)$ at some $p = p_1$ implies that the superior and the inferior limits at $t \to \infty$ must be different, which, in turn, implies the existence of a subsequence convergent to the non-zero limit given by $\limsup_{t\to\infty} \mathbf{P}_E(t,p_1) > 0$.

Similarly, we define the upper cycle erasure threshold,

$$p_E^1 = \inf\left\{p \in [0,1] : \lim_{t\to\infty} \mathbf{P}_A(t,p) = 0\right\}, \tag{3.4}$$

as the smallest p such that open subgraphs preserve the full-rank homology group with probability approaching one in the limit of the sequence.

Existence of a homologically non-trivial cycle not covered by open edges implies that closed edges must cover a conjugate codeword, a non-trivial co-cycle. The related threshold on an infinite graph can be interpreted in terms of a transition dual to percolation, proliferation of the boundaries at the complementary edge configuration, with all closed edges replaced by open edges, and v.v., so that the open edge probability becomes $\bar{p} = 1-p$. On a locally planar graph, like a tiling of a two-dimensional manifold, the dual transition maps to the usual percolation on the dual graph.

We also notice that the usual erasure threshold p_E for a family (or a sequence) of quantum codes corresponds to a non-zero probability of an *erasure*, a configuration where a codeword is covered by erased qubits. For a CSS code, this implies a non-zero probability that either an X- or a Z-type codeword be covered. For codes $\mathcal{Q}_t$ associated with covering maps $f_t : \mathcal{H} \to \mathcal{G}_t$ in the sequence $(\mathcal{G}_t)_{t\in\mathbb{N}}$, the conventional erasure threshold can be found in terms of the thresholds for cycles and co-cycles,

$$p_E = \min(p_E^0, 1 - p_E^1). \tag{3.5}$$

The following lower bound constructed using a Peierls-style counting argument

is adapted from Ref. [19]:

Statement 4 *Consider a sequence of finite graphs $(\mathcal{G}_t)_{t\in\mathbb{N}}$ with a common covering graph $\mathcal{H}$. Let $\Delta_{\max}$ be the maximum degree of $\mathcal{H}$, and assume that for some $t_0 > 0$, the injectivity radius r_t associated with the maps $f_t : \mathcal{H} \to \mathcal{G}_t$ at $t \geq t_0$ scales at least logarithmically with the number of edges n_t, $r_t \geq A \ln n_t$, with some $A > 0$. The cycle erasure threshold for the corresponding sequence of CSS codes $(\mathcal{Q}_t)_{t\in\mathbb{N}}$ satisfies the lower bound $p_E^0 \geq e^{-1/(2A)}/(\Delta_{\max} - 1)$.*

It follows from the fact that $\mathcal{Q}_t = \mathrm{CSS}(J_t, K_t)$, where J_t is the vertex-edge incidence matrix of $\mathcal{G}_t$, with row weights given by the vertex degrees, and Lemma 1.

We would like to ensure that the conventional erasure threshold (3.5) also be non-trivial, which requires that $p_E^1 < 1$. To construct such an upper bound, which becomes a lower bound in terms of $\bar{p} = 1-p$ in the dual representation, it is sufficient [19] that rows of the trivial-cycle–edge adjacency matrix K_t have bounded weights, and that the distance d_{Xt} diverges logarithmically or faster with n_t. Notice that here we do not rely on Lemma 2 which gives a rather weak lower bound for the distance but, instead, directly assume desired scaling of the minimum weight d_{Xt} of a non-trivial co-cycle with n_t. We have

Statement 5 *Consider a sequence of finite graphs $(\mathcal{G}_t)_{t\in\mathbb{N}}$ with a common covering graph $\mathcal{H}$, with the cycle group $\mathcal{C}(\mathcal{H})$ generated by cycles of weight not exceeding $\omega > 1$. Further, assume that the minimum weight $d_{Xt} \equiv d_X(\mathcal{H}; f_t)$ of a non-trivial co-cycle associated with the map $f_t : \mathcal{H} \to \mathcal{G}_t$ grows at least logarithmically with the number of edges n_t, $d_{Xt} \geq A' \ln n_t$, for sufficiently large $t \geq t_0'$ and some $A' > 0$. The upper erasure threshold for the corresponding sequence of CSS codes $(\mathcal{Q}_t)_{t\in\mathbb{N}}$ satisfies the bound*

$1 - p_E^1 \geq e^{-1/A'}/(\omega - 1)$.

Let us now relate the cycle erasure threshold p_E^0 with the bulk percolation threshold. Most generally, it serves as an upper bound:

Theorem 6 *Consider a sequence of finite graphs $(\mathcal{G}_t)_{t\in\mathbb{N}}$ covered by an infinite graph $\mathcal{H}$. Then, $p_E^0 \leq p_c(\mathcal{H})$.*

Proof. If $p_c(\mathcal{H}) = 1$, the statement of the theorem is trivial. In the following, assume $p_c(\mathcal{H}) < 1$ and take p such that $p_c(\mathcal{H}) < p < 1$. For some $t \in \mathbb{N}$, a chosen $v' \in \mathcal{V}_\mathcal{H}$ and $v \equiv f_t(v')$, we connect percolation on $\mathcal{H}$ and on $\mathcal{G}_t$ using a set-up similar to invasion percolation [56]. Namely, we start with single-site zeroth generation clusters $\mathcal{K}_v^{(0)} = \{v\} \subset \mathcal{V}_t$ and $\mathcal{K}_{v'}^{(0)} = \{v'\} \subset \mathcal{V}_\mathcal{H}$, with no edges labeled open or closed. Given a generation-j cluster $\mathcal{K}_{v'}^{(j)} \subset \mathcal{V}_\mathcal{H}$, every previously unlabeled edge adjacent to a vertex in $\mathcal{K}_{v'}^{(j)}$ is labeled open with independent probability p and otherwise closed. The next generation cluster $\mathcal{K}_{v'}^{(j+1)}$ is formed by adding any vertices connected to those in $\mathcal{K}_{v'}^{(j)}$ by newly open edges. Let us denote by $P_j(p;\mathcal{H})$ the probability that the process reaches set j and can be continued, i.e., there is one or more unlabeled edges incident on the j-th generation cluster. Clearly, $P_0(p;\mathcal{H}) = 1$ and $P_j(p;\mathcal{H})$ is strictly decreasing as a function of j, with $\lim_{j\to\infty} P_j(p;\mathcal{H}) = \theta_{v'}(p;\mathcal{H})$.

Let us now look at thus constructed percolation process on $\mathcal{G}_t$. As long as the image of no vertex connected to $\mathcal{K}_{v'}^{(j)}$ by a so far unlabeled edge coincides with the image of a vertex in $\mathcal{K}_{v'}^{(j)}$ (we call such a cluster "flat"), we can use the map f_t to make the labels on $\mathcal{G}_t$ match those on $\mathcal{H}$. Clearly, all clusters are flat for $j < r_t$, the injectivity radius; for such j the probabilities that the percolation process may be continued match exactly on the two graphs, $P_j(p;\mathcal{G}_t) = P_j(p;\mathcal{H})$. On the other hand, $P_j(p;\mathcal{G}_t) = 0$ for

$j \geq |\mathcal{V}_t|$. The percolation processes necessarily decouple whenever a cluster $\mathcal{K}_{v'}^{(j)}$ ceases to be flat, i.e., there be an unlabeled edge on $\mathcal{G}_t$ connecting a pair of vertices in $\mathcal{K}_v^{(j)} \subset \mathcal{V}_t$. Given such a cluster, we can assign the remaining unlabeled edges on $\mathcal{G}_t$ all at once; the resulting open subgraph of $\mathcal{G}_t$ contains a homologically non-trivial cycle with probability greater than or equal to p. At the same time, the cluster $\mathcal{K}_{v'}^{(j)} \subset \mathcal{V}_{\mathcal{H}}$ is removed from the percolation process on $\mathcal{H}$. Since it is not certain that a descendant of a given cluster be infinite, we get the lower bound

$$\mathbb{P}(\mathcal{K}_v \text{ contains a non-trivial cycle}) \geq p\,\theta_{v'}(p;\mathcal{H}), \tag{3.6}$$

which is positive for any $p > p_{\mathrm{c}}$, thus $p_E^0 \leq p_{\mathrm{c}}$. ■

This includes the case where the sequence of the injectivity radii remains bounded (no weak convergence to $\mathcal{H}$), in which case, obviously, $p_E^0 = 0$. More precise results for p_E^0 are available with additional assumptions, including the scaling of the injectivity radius with the logarithm of the graph size:

Theorem 7 *Consider a sequence of finite transitive graphs $(\mathcal{G}_t)_{t\in\mathbb{N}}$ covered by an infinite graph $\mathcal{H}$. If the homological distance d_{Zt} scales sublogarithmically with graph size, $\lim\limits_{t\to\infty} \dfrac{d_{Zt}}{\ln n_t} = 0$, then $p_E^0 = 0$.*

Proof. To set up independent erasure events, cut $\mathcal{G}_t$ into non-overlapping regions, images of non-overlapping balls on $\mathcal{H}$ of radius $\rho_t \equiv 1 + \lfloor d_{Zt}/2 \rfloor$. Given the maximum graph degree $\Delta_{\max}$, we can cut out at least

$$N_t \geq |V_t|/|\mathcal{B}_0(2\rho_t, \mathcal{G}_t)| > |V_t|/\Delta_{\max}^{2+d_{Zt}}$$

such balls. By transitivity of $\mathcal{G}_t$ and Lemma 2, each ball contains a homologically non-trivial cycle of length d_{Zt}, which is open with probability $P_1 \geq p^{d_{Zt}}$. Now, the

probability that a homology is covered in *none* of the N_t balls can be upper bounded as

$$\begin{aligned} P_{\text{none}} &= [1-P_1]^{N_t} \leq [1-p^{d_{Zt}}]^{N_t} \leq \exp(-N_t p^{d_{Zt}}) \\ &< \exp\left(-|V_t|/\Delta_{\max}^2\, e^{-d_{Zt}(|\ln p|+\ln\Delta_{\max})}\right), \end{aligned} \tag{3.7}$$

which is guaranteed to converge to zero for any $p > 0$ since d_{Zt} scales sublogarithmically with $|V_t|$. (Notice that $|V_t| \geq 2n_t/\Delta_{\max}$ by a version of the hand-shaking lemma.) ■

Notice that the requirement of transitivity for the graphs $\mathcal{G}_{Zt}$ can be relaxed a bit, namely, by assuming that the number of vertex classes [defined by distinct vertex orbits connected by elements of $\mathrm{Aut}(\mathcal{G}_t)$] remains uniformly bounded for the graphs $\mathcal{G}_t$. In that case, the balls need to be taken of radius $\rho_t = \lfloor d_{Zt}/2 \rfloor + m$, where m is the maximum number of vertex classes. The proof is completed with the following lemma:

Lemma 8 *Consider a connected graph $\mathcal{H}$, with $m \geq 1$ vertex classes. Any ball of radius m contains representative(s) of all classes.*

Proof. Consider a class connectivity graph $\mathcal{G}$ corresponding to $\mathcal{H} = (\mathcal{V}, \mathcal{E})$, with m vertices (one per class) and an edge between two vertices if $\mathcal{H}$ contains an edge between a pair of vertices in these classes. Necessarily, $\mathcal{G}$ is connected. Further, given a vertex $v \in \mathcal{V}$, any spanning tree on $\mathcal{G}$ can be lifted to a tree on $\mathcal{H}$ that contains v; such a tree contains a representative from every vertex class. Further, the diameter of the tree cannot exceed m; such a tree is contained in a ball $\mathcal{B}(v, m; \mathcal{H})$. The proof is complete since the choice of v is arbitrary. ■

Theorem 9 *Consider a sequence of finite graphs $(\mathcal{G}_t)_{t\in\mathbb{N}}$ covered by an infinite quasi-transitive graph $\mathcal{H}$. If the injectivity radius scales superlogarithmically with the graph size, $\lim_{t\to\infty} \dfrac{r_t}{\ln n_t} = \infty$, then $p_E^0 = p_{\mathrm{c}}$.*

Proof. Only a cluster with $s \geq d_{Zt} > r_t$ vertices can cover a homology. For a graph $\mathcal{G}$, let $M_v(s;\mathcal{G})$ denote the probability that vertex v is in an open cluster with exactly s vertices on $[\mathcal{G}]_p$. On the quasi-transitive graph $\mathcal{H}$, this probability has an exponential bound, $M_v(s;\mathcal{H}) < M(s) \equiv e^{-\gamma(p)s}$, for some $\gamma(p)$ non-zero in the subcritical region, $\gamma(p) > 0$ for $p < p_{\rm c}$ [2]. Note also $\sum_{s\geq 1} M_v(s;\mathcal{G}) = 1$ on any finite graph; below percolation threshold this is also true for infinite graphs. Also, for any $v \in \mathcal{V}_t$, finding a cluster of size $s \leq r_t$ attached to v on $\mathcal{G}_t$ has the same probability as that attached to a vertex $v'(v)$ from the fiber of v on $\mathcal{H}$. Use the union bound for the probability of finding a cluster of size $r_t + 1$ or larger on $\mathcal{G}_t$,

$$\begin{aligned}
P_{\rm one} &\leq \sum_{v\in\mathcal{V}_t}\sum_{s>r_t} s^{-1} M_v(s;\mathcal{G}_t) \\
&< \sum_{v\in\mathcal{V}_t}\sum_{s>r_t} M_v(s,\mathcal{G}_t) \\
&= \sum_{v\in\mathcal{V}_t}\left(1 - \sum_{1\leq s\leq r_t} M_v(s;\mathcal{G}_t)\right) \\
&= \sum_{v\in\mathcal{V}_t}\left(1 - \sum_{1\leq s\leq r_t} M_{v'(v)}(s;\mathcal{H})\right) \\
&= \sum_{v\in\mathcal{V}_t}\sum_{s>r_t} M_{v'(v)}(s;\mathcal{H}) \\
&< |\mathcal{V}_t| \sum_{s>r_t} e^{-\gamma(p)s} = \frac{|V_t| e^{-\gamma(p) r_t}}{e^{\gamma(p)} - 1},
\end{aligned} \tag{3.8}$$

which goes to zero with $t \to \infty$ whenever $\gamma(p) > 0$ since r_t is assumed to be superlogarithmic in $n_t \geq |\mathcal{V}_t| - 1$. This proves $p_E^0 \geq p_{\rm c}$; the statement of the Theorem is obtained with the help of Theorem 6. ■

Information about the other threshold, p_E^1, can be obtained in the planar case with the help of duality:

Corollary 10 *Let $\mathcal{H}$ and $\widetilde{\mathcal{H}}$ be a pair of mutually dual infinite quasitransitive planar graphs. Consider a sequence of finite graphs $(\mathcal{G}_t)_{t\in\mathbb{N}}$ weakly convergent to $\mathcal{H}$, a cover of the graphs in the sequence. Then,*

(**i**) $p_E^1 \geq 1 - p_c(\widetilde{\mathcal{H}})$. *In addition,*

(**ii**) *if the graphs $\mathcal{G}_t$ in the sequence are transitive, $t \in \mathbb{N}$, and the injectivity radius grows sublogarithmically with the graph size, then $p_E^1 = 1$;*

(**iii**) *if the injectivity radius grows superlogarithmically, then $p_E^1 = 1 - p_c(\widetilde{\mathcal{H}})$.*

Proof. Since $\widetilde{\mathcal{H}}$ is quasitransitive, it has a finite maximum degree, which is the maximum size of a face of $\mathcal{H}$. Thus, with injectivity radius large enough, f_t must be invertible on the union of any face and its adjacent faces on $\mathcal{H}$. This guarantees that (with t sufficiently large, $t > t_0$), $\mathcal{G}_t$ be locally planar, so that we can construct the locally planar dual graph $\widetilde{\mathcal{G}}_t$ whose cover is $\widetilde{\mathcal{H}}$. Further, for any open edge configuration, the ranks of the homology groups on the open subgraph of $\mathcal{G}_t$ and on the closed subgraph of $\widetilde{\mathcal{G}}_t$ add to k_t, the number of inequivalent homologically non-trivial cycles on $\mathcal{G}_t$ [Eq. (2.8)]. Thus, the two erasure thresholds are simply interchanged by duality, $\tilde{p}_E^1 = 1 - p_E^0$ and $\tilde{p}_E^0 = 1 - p_E^1$, so the inequality $p_E^1 \geq 1 - p_c(\widetilde{\mathcal{H}})$ follows immediately from Theorem 6.

The identities in (**ii**) and (**iii**) similarly follow from Theorems 7 and 9 with the help of Lemmas 1 and 2 which guarantee that the injectivity radii on the sequence of mutually dual graphs scale simultaneously in a sub-logarithmic, logarithmic, or super-logarithmic fashion. ■

Notice that for a superlogarithmic scaling of the injectivity radius, the graph must be amenable, in which case $p_u(\mathcal{H}) = p_c(\mathcal{H})$. We also believe that under conditions of the Corollary, the duality gives $p_u(\mathcal{H}) = 1 - p_c(\widetilde{\mathcal{H}})$, see Eq. (2.22), although we

only found the proof for the case where the graph $\mathcal{H}$ is transitive [27]. Whenever such a duality relation holds, the upper cycle erasure threshold is bounded below by the uniqueness threshold, $p_E^1 \geq p_{\mathrm{u}}(\mathcal{H})$; with superlogarithmic scaling of the injectivity radius, the sequence of thresholds collapses to a single point, $p_E^0 = p_E^1 = p_{\mathrm{c}}(\mathcal{H}) = p_{\mathrm{u}}(\mathcal{H})$.

These results leave out an important case of percolation with logarithmic distance scaling. It is easy to see that logarithmic distance scaling does not necessarily imply that p_E^0 and $p_{\mathrm{c}}(\mathcal{H})$ be equal:

Example 11 (Anisotropic square-lattice toric codes) *Consider a sequence of tori $\mathcal{G}_t = \mathcal{T}_{L_x(t),L_y(t)}$ obtained from the infinite square lattice $\mathcal{H}$ by identifying the vertices at distances $L_x(t)$ and $L_y(t)$ along the edges in x and y directions, respectively. For some $A > 0$, consider the scaling $L_x(t) = t$, $L_y(t) = e^{t/A}/(2t)$. This gives $d_{Zt} = t$ and $n_t = e^{t/A}$, so that $d_{Zt} = A \ln n_t$. The cycle erasure threshold p_E^0 for this graph sequence satisfies $e^{-1/A}/3 < p_E^0 \leq e^{-1/A}$.*

The upper bound follows from considering $L_y(t)$ independent non-trivial cycles of length t, while the lower bound is given by Statement 4. In comparison, for edge percolation on infinite square lattice, $p_{\mathrm{c}} = 1/2$.

In addition to Example 11, in Sec. 4 we give numerical evidence that $p_E^0 < p_{\mathrm{c}}(\mathcal{H})$ for several families of hyperbolic codes based on regular $\{f, d\}$ tilings of the hyperbolic plane (here $2df > d + f$; these are known to have a finite asymptotic rate $R = 1 - 2/d - 2/f$).

3.2 Erasure rate thresholds

Logarithmic scaling of the minimum distance d_{Zt} associated with the first homology group is the largest one may hope for in the important case when the covering graph $\mathcal{H}$ is non-amenable. We specifically focus on the case of a graph sequence with *extensive homology rank* scaling, i.e., where the associated codes have an asymptotically finite rate, $R \equiv \lim_{t\to\infty} k_t/n_t > 0$. For such graph sequences, we also consider the expected dimension of the erased subspace per edge, or the *erasure rate*,

$$\mathbf{R}_E(t,p) \equiv n_t^{-1}\, \mathbb{E}_p\big(\operatorname{rank} H_1(f_t,p)\big). \tag{3.9}$$

An analogous quantity was analyzed in detail by Delfosse and Zémor [15]. Unlike the probabilities $\mathbf{P}_E$ and $\mathbf{P}_A$, the erasure rate $\mathbf{R}_E$ is a bulk quantity which can be used to define a thermodynamical transition in the usual sense. For any $t \in \mathbb{N}$, the erasure rate $\mathbf{R}_E(t,p)$ is a monotonously increasing function of $p \in [0,1]$, bounded by the values at the ends of the interval,

$$0 \le \mathbf{R}_E(t,p) \le R_t \equiv k_t/n_t \le 1. \tag{3.10}$$

Let us now consider the thresholds associated with the erasure rate (3.9). We define the lower p_H^0 and the upper p_H^1 critical points as the values of p where $\mathbf{R}_E(t,p)$ in the limit of large t starts to deviate from 0 and from R, respectively:

$$p_H^0 = \sup\{p \in [0,1] : \lim_{t\to\infty} \mathbf{R}_E(t,p) = 0\}, \tag{3.11}$$

$$p_H^1 = \inf\{p \in [0,1] : \lim_{t\to\infty} \mathbf{R}_E(t,p) = R\}. \tag{3.12}$$

We call these, respectively, the lower and the upper *homological* thresholds. Evidently, $p_E^0 \le p_H^0 \le p_H^1 \le p_E^1$. The critical point p_H^0 was discussed in Refs. [14, 15]. Our first

result, an analogue of the corresponding inequality for the Ising model, Eq. (34) in Ref. [32], gives a lower bound on the gap between the two homological thresholds:

Theorem 12 *Consider a sequence of finite graphs $(\mathcal{G}_t)_{t\in\mathbb{N}}$ weakly convergent to an infinite graph $\mathcal{H}$, a cover of the graphs in the sequence, with rate-R extensive homology rank. Then there is a finite gap between the two homological thresholds,*

$$p_H^1 - p_H^0 \geq R. \tag{3.13}$$

Proof. Let $k_t = \operatorname{rank} H_1(f_t)$ be the number of non-trivial independent cycles on $\mathcal{G}_t$. Consider any open edge configuration on $\mathcal{G}_t$, with homology rank $k_t' \leq k_t$, and another edge configuration obtained by removing some open edges, with homology rank $k_t'' \leq k_t'$. Such a change in homology requires removing at least $\Delta k_t = k_t' - k_t''$ open edges. Considering these as random edge configurations at $p' > p_H^1$ and $p'' < p_H^0$, averaging, and dividing by the total number of edges n_t, we obtain

$$p' - p'' \geq \mathbf{R}_E(t, p') - \mathbf{R}_E(t, p'');$$

in the limit $t \to \infty$ this becomes $p' - p'' \geq R$. Taking infimum over $p' > p_H^1$ and supremum over $p'' < p_H^0$, we obtain the claimed inequality. ■

Second, we prove an "easy" inequality relating the lower homological threshold with the percolation threshold on the covering graph:

Theorem 13 *For a sequence of finite graphs $(\mathcal{G}_t)_{t\in\mathbb{N}}$ weakly convergent to an infinite graph $\mathcal{H}$, a cover of the graphs in the sequence with extensive homology rank, $p_{\mathrm{c}}(\mathcal{H}) \leq p_H^0$.*

Proof. Take $p > p_H^0$, then the limit in Eq. (3.11) is either strictly positive or does not exist. In either case, since terms in the sequence are bounded, $\mathbf{R}_E(t, p) < 1$,

the superior limit $f_p \equiv \limsup_{t\to\infty} \mathbf{R}_E(t,p)$ exists and is strictly positive, $f_p > 0$ at $p > p_H^0$. This implies the existence of a convergent subsequence, e.g., specified by an increasing sequence of indices $(t_j)_{j\in\mathbb{N}}$ such that $\lim_{j\to\infty} \mathbf{R}_E(t_j,p) = f_p$.

Because of the existence of the limit, whenever $f_p > 0$, for any $\epsilon > 0$ and a sufficiently large j, clusters covering homologically non-trivial cycles are expected to occupy at least $(f_p - \epsilon)n_t$ edges, where $t \equiv t_j$. Thus, if we choose $\epsilon = f_p/2$, a cluster $K_v \subset [\mathcal{G}_t]_p$ connected to a randomly chosen vertex $v \in \mathcal{V}_t$ covers a homologically non-trivial cycle with probability $P_{\text{non-triv}} \geq f_p n_t/(2|\mathcal{V}_t|)$. Using a map like that in the proof of Theorem 6, at sufficiently large t, a cluster covering a non-trivial cycle on $[\mathcal{G}_t]_p$ corresponds to an infinite cluster on $[\mathcal{H}]_p$, which gives

$$\theta_v(p) \geq \lim_{j\to\infty} f_p n_{t_j}/(2|\mathcal{V}_{t_j}|) \geq f_p/2 > 0,$$

thus $p > p_{\text{c}}(\mathcal{H})$. ■

The remaining analytical result is obtained with the help of the usual duality between locally planar graphs, and is therefore limited to planar graphs $\mathcal{H}$:

Theorem 14 *Let $\mathcal{H}$ and $\widetilde{\mathcal{H}}$ be a pair of infinite mutually dual transitive planar graphs. Consider a sequence of finite graphs $(\mathcal{G}_t)_{t\in\mathbb{N}}$ weakly convergent to $\mathcal{H}$, a cover of the graphs in the sequence with extensive homology rank. Then,*

$$\textbf{(i)}\ p_H^0 = p_{\text{c}}(\mathcal{H}), \quad \textbf{(ii)}\ p_H^1 = 1 - p_{\text{c}}(\widetilde{\mathcal{H}}) = p_{\text{u}}(\mathcal{H}). \tag{3.14}$$

This is an easy consequence of two previous results: the expression [15] for the expected homology rate in terms of the average inverse cluster sizes on the graph and its dual, and the exponential decay [2, 28] of the size of finite clusters away from the percolation point on transitive graphs.

Proof. As in the proof of Corollary 10, at sufficiently large t the graph $\mathcal{G}_t = (\mathcal{V}_t, \mathcal{E}_t)$ is necessarily locally planar, which implies the existence of the corresponding dual graph $\widetilde{\mathcal{G}}_t = (\widetilde{\mathcal{V}}_t, \widetilde{\mathcal{E}}_t)$, with the dual-graph sequence weakly convergent to the dual infinite graph $\widetilde{\mathcal{H}}$.

The proof relies on the relation [15] between the expected homology rank of the open subgraph and the expected inverse cluster sizes on an open subgraph of $\mathcal{H}$ and a closed subgraph of $\widetilde{\mathcal{H}}$. While the argument goes back to the work of Sykes and Essam [53], we give a complete derivation here. Consider a configuration of open/closed edges on $[\mathcal{G}_t]_p$ with $E' \le n_t \equiv |\mathcal{E}_t|$ open edges, K' clusters, and the cycle group of rank $C' = C_{\rm triv} + k'$, where k' is the number of non-trivial basis cycles. According to Euler's theorem, $K' = |\mathcal{V}_t| - E' + C'$. On the other hand, duality matches any simple trivial cycle on $\mathcal{G}_t$ to a cut on the dual graph $\widetilde{\mathcal{G}}_t$, which gives $C_{\rm triv} = \tilde{K}' - 1$, with $\tilde{K}'$ being the number of clusters on the dual graph in the dual edge configuration, with open and closed edges interchanged. This gives

$$k' = K' - \tilde{K}' + E' - |\mathcal{V}_t| + 1.$$

Taking the average over the edge configurations on $[\mathcal{G}_t]_p$ we obtain for $k_p^{(t)} \equiv \mathbb{E}_p\big(\text{rank}\, H_1(f_t, p)\big)$,

$$k_p^{(t)} \;=\; \sum_{v\in\mathcal{V}_t} \kappa_v(p;\mathcal{G}_t) - \sum_{v\in\widetilde{\mathcal{V}}_t} \kappa_v(\bar{p};\widetilde{\mathcal{G}}_t) + pn_t - |\mathcal{V}_t| + 1.$$

Here $\kappa_v(p;\mathcal{G}_t) \equiv \mathbb{E}_p\left(|K_v|^{-1}\right)$ is the expected inverse size of a cluster containing vertex v on $[\mathcal{G}_t]_p$, and $\kappa_v(\bar{p};\widetilde{\mathcal{G}}_t)$ is the corresponding quantity on the dual graph, averaged over the dual edge configurations, which is equivalent to $\bar{p} = 1-p$. Introducing the corresponding vertex-average quantities, e.g., $\kappa(p;\mathcal{G}_t) \equiv |\mathcal{V}_t|^{-1}\sum_{v\in\mathcal{V}_t}\kappa_v(p;\mathcal{G}_t)$, we get

$$k_p^{(t)} = |\mathcal{V}_t|\kappa(p;\mathcal{G}_t) - |\widetilde{\mathcal{V}}_t|\kappa(1-p;\widetilde{\mathcal{G}}_t) + pn_t - |\mathcal{V}_t| + 1.$$

To obtain the asymptotic erasure rate (3.9) we divide the obtained result by n_t and notice that very large clusters give no contribution to the total while (at sufficiently large t) any finite cluster on $[\mathcal{H}]_p$ has the same probability as an equivalent cluster on $[\mathcal{G}_t]_p$. Further, assuming the transitive graphs $\mathcal{H}$ and $\widetilde{\mathcal{H}}$ of degrees d and f, respectively, the graphs $\mathcal{G}_t$ and $\widetilde{\mathcal{G}}_t$ respectively have the same degrees, and the hand-shaking lemma gives $|\mathcal{V}_t| = 2n_t/d$, $|\widetilde{\mathcal{V}}_t| = 2n_t/f$. This proves both the existence and the value of the following limit at any p,

$$\begin{aligned} \mathbf{R}_E(p) &\equiv \lim_{t\to\infty} \mathbf{R}_E(t,p) \\ &= \frac{2}{d}\kappa(p;\mathcal{H}) - \frac{2}{f}\kappa(\bar{p};\widetilde{\mathcal{H}}) + p - \frac{2}{d}. \end{aligned} \tag{3.15}$$

Finally, we notice that for non-amenable transitive graphs $\mathcal{H}$ and $\widetilde{\mathcal{H}}$, the quantities $\kappa(p;\mathcal{H})$ and $\kappa(\bar{p};\widetilde{\mathcal{H}})$ are analytic functions of p in the vicinity of any $p \in (0,1)$ such that $p \neq p_{\mathrm{c}}(\mathcal{H})$ and $\bar{p} \neq p_{\mathrm{c}}(\widetilde{\mathcal{H}})$, respectively [2, 28]. Thus, the r.h.s. of Eq. (3.15) is an analytic function of p for

$$p \in (0,1) \setminus \{p_{\mathrm{c}}(\mathcal{H}), 1 - p_{\mathrm{c}}(\widetilde{\mathcal{H}})\},$$

where $1 - p_{\mathrm{c}}(\widetilde{\mathcal{H}}) = p_{\mathrm{u}}(\mathcal{H}) > p_{\mathrm{c}}(\mathcal{H})$. On the other hand, $\mathbf{R}_E(p)$ cannot be analytic in the lower and upper homological thresholds $0 < p_H^0 < p_H^1 < 1$, which gives the two equalities. ■

Notice that in Theorem 14, the lower and the higher homological thresholds, respectively, are actually associated with the percolation and the uniqueness thresholds on the infinite graph $\mathcal{H}$. We believe this is not a coincidence, and put forward

Conjecture 15 *Consider a sequence of finite graphs $(\mathcal{G}_t)_{t\in\mathbb{N}}$ weakly convergent to a quasitransitive infinite graph $\mathcal{H}$, a cover of the graphs in the sequence with extensive*

homology rank. Then,

$$(\mathbf{i})\ p_H^0 = p_{\mathrm{c}}(\mathcal{H}), \quad (\mathbf{ii})\ p_H^1 = p_{\mathrm{u}}(\mathcal{H}). \tag{3.16}$$

Such a result makes sense, since neither the percolation nor the uniqueness thresholds can be seen locally, by examining a finite subgraph of $\mathcal{H}$. Similarly, the homological transitions require changes in cycles of length exceeding the injectivity radius, which diverges without a bound.

Chapter 4

Numerical Results and Methods

In addition to analytical results, we also evaluated the erasure and the percolation thresholds numerically for several families of locally planar hyperbolic codes, the euclidean square lattice toric codes and random degree 5 graphs. Each family corresponds to a particular infinite graph $\mathcal{H}_{f,d}$, regular tiling of the hyperbolic or euclidean plane, parameterized by the Schläfli symbol $\{f, d\}$, such that it follows the hyperbolic or euclidean relations as follows,

$$1/f + 1/d \begin{cases} < 1/2 \implies \text{hyperbolic} \\ = 1/2 \implies \text{euclidean} \\ > 1/2 \implies \text{spherical} \end{cases} . \tag{4.1}$$

In such a graph, d identical f-gons meet at each vertex. The finite graphs are constructed [49, 47, 8] as finite quotients of the corresponding graph $\mathcal{H}_{f,d}$ with respect to subgroups of the symmetry group.

4.1 Graph Construction

The parameters of the graphs used in the calculations are listed in Tab. 4.1, where $\{f, d\}$ is the Schläfli symbol of the corresponding tiling, n is the number of edges, and d_Z and d_X, respectively, are the distances of the corresponding CSS codes. The smaller graphs with $n < 10^3$ edges are from N. P. Breuckmann [9]. We generated the remaining graphs with a custom `GAP` [24] program, which constructs coset tables of freely presented groups obtained from the infinite van Dyck group $D(d, f, 2) = \langle a, b | a^d, b^f, (ab)^2 \rangle$ [here a and b are group generators, while the remaining arguments are *relators* which correspond to imposed conditions, $a^d = b^f = (ab)^2 = 1$] by adding one more relator obtained as a pseudo random string of generators to obtain a suitable finite group $\mathcal{D}$, a quotient of the original infinite group $D(d, f, 2)$. Then, the vertices, edges, and faces are enumerated by the right cosets with respect to the subgroups $\langle a \rangle$, $\langle ab \rangle$, and $\langle b \rangle$, respectively. The vertex-edge and face-edge incidence matrices J and K are obtained from the coset tables. Namely, non-zero matrix elements are in the positions where the corresponding pair of cosets share an element. Finally, the distance d_Z of the CSS code $\mathrm{CSS}(J, K)$ was computed using the covering set algorithm, which has the advantage of being extremely fast when the distance is small [18, 20], and additionally verified by comparing the number of cycles through a given vertex on the finite graph $\mathcal{G}$ and on a sufficiently large subgraph of the infinite covering graph $\mathcal{H}_{f,d}$. The distance d_X is obtained by interchanging the CSS generator matrices J and K, which is equivalent to considering the corresponding dual graph.

After creating each graph and calculating its distance, we needed to determine which graphs are of the right type to calculate percolation transitions. This is because

we needed a set of graphs which have the same, or nearly the same, finite size scaling factor, the ratio $d/\ln n$ of the distance to the logarithm of the number of edges. In order to determine this, we took into account the number of edges, n, and its distance.

Each graph was labeled as either optimal or non-optimal. An *optimal graph* is a graph such that no graph of a smaller size has a distance greater or equal to it. This set is small since it is limited to one graph per distance, at best, and the difficulty in finding optimal graphs grows exponentially with distance. We are also not sure if the graphs we label as optimal are truly optimal, since there may be a smaller graph with the same distance we just did not find.

Two different sets of graphs were kept. One set was used to calculate p_c and p_G, the values which do not depend on the homological cycles. The second set was used to calculate p_E^0, which is dependent on the homological cycles. Both sets only contain graphs with n larger than 500, $d_Z > f$, and $d_X > d$. This is because we want larger graphs, which can also function as proper codes.

The first set is composed of the 20 largest graphs for each $\{f, d\}$, if we had that many. The second set is composed of only the optimal graphs. This greatly limited which families of codes we could analyze, since multiple families had less than three optimal graphs. Looking at Tabs. 4.1, 4.2, 4.3 and 4.4 you can see graphs of the type $\{4, 7\}$ and $\{5, 6\}$ had less than three optimal graphs and thus their thresholds were not calculated.

To better understand the difference of hyperbolic codes, we also calculated the percolation transitions for random graphs with constant degree. In particular we took each vertex to have degree 5 and use the Schläfli symbol $\{r, 5\}$ to denote such graphs.

	n	720	864	2448	6144	8640	18144	18216	19584	23760	24360	24576	25308	25920	27360	29760	31200	32256	32928	35280	36288	38880	40320	41040	46080	46656
$\{4,6\}$	d_Z	**8**	8	8	**10**	8	10	10	8	10	10	10	10	10	10	10	10	10	8	10	10	10	10	8	10	**12**
$\{6,4\}$	d_X	8	**10**	**12**	12	**14**	12	14	14	12	14	12	14	10	12	14	12	14	14	10	14	12	14	10	12	12
	n	46800	48576	50616	51888	52416	58800	62400																		
$\{4,6\}$	d_Z	8	10	10	11	10	11	12																		
$\{6,4\}$	d_X	12	14	14	14	12	15	12																		
	n	504	648	768	864	1080	1224	1944	2016	2448	2592	3072	3240	4032	4320	5616	5832	6000	6072	6144	7344	14880	16848	18216	25944	32256	
$\{3,8\}$	d_Z	**6**	6	6	6	6	6	6	**8**	8	6	8	8	8	8	8	8	8	8	8	8	8	**9**	**10**	9	10
$\{8,3\}$	d_X	14	14	**16**	12	16	15	12	**18**	16	18	18	18	18	16	16	18	**22**	20	18	18	22	20	**24**	21	24
	n	660	1800	1920	3420	4860	5760	7440	9600	10240	11520	12180	14880	17100	19200	23040	29400	34440	37500	38880	43200	57600	58240	58800	60900	61440	
$\{4,5\}$	d_Z	8	**10**	10	10	**12**	10	12	12	12	10	12	12	**14**	12	12	14	14	14	12	14	10	13	14	12	12
$\{5,4\}$	d_X	**10**	10	**12**	**14**	12	10	14	14	14	10	14	14	**16**	14	15	**17**	16	16	16	16	10	15	**18**	16	12
	n	960	2520	3840	4800	4860	5040	6840	7560	7680	9600	9720	12180	14580	15120	15360	17100	19200	24360	25200	29400	29760	30720	34200	37800		
$\{6,5\}$	d_Z	**7**	**8**	8	**10**	8	10	10	10	10	8	10	8	10	10	8	8	10	10	10	9	10	8	10	10		
$\{5,6\}$	d_X	6	6	**8**	8	7	7	6	8	8	8	7	6	6	8	8	8	8	8	8	8	8	8	8	**10**		
	n	900	4800	9600	9720	10800	11520	14400	15360	17220	18750	19440	19800	21600	29120	29400	30450	38880	40960	51330	52800	56730	58240				
$\{5,5\}$	d_Z, d_X	**8**	**10**	10	10	9	8	8	**11**	10	10	10	10	11	**12**	10	12	10	12	12	10	11	12				
	n	2688	5376	7644	9828	12180	21504	34440	39732	43008	58240																
$\{7,4\}$	d_Z	**11**	**12**	10	12	**13**	12	12	10	12	**14**																
$\{4,7\}$	d_X	6	6	**8**	8	8	8	8	**10**	10	8																
	n	546	672	4914	5376	6090	17220	19866																		
$\{3,7\}$	d_Z	**7**	**8**	**10**	**12**	10	12	12																		
$\{7,3\}$	d_X	14	**16**	**24**	24	20	**28**	26																		

Table 4.1: Parameters of the hyperbolic graphs used to calculate critical p values. Given a Schläfli symbol $\{f, d\}$, finite graphs $\mathcal{G}$ and their dual graphs $\widetilde{\mathcal{G}}$ are parameterized by the number of edges n; they have $2n/d$ and $2n/f$ vertices, respectively, and the first homology groups of rank $k = 2 + (1 - 2/d - 2/f)n$. Distances d_Z and d_X are the lengths of the shortest homologically non-trivial cycles on $\mathcal{G}$ and $\widetilde{\mathcal{G}}$, respectively. Numbers in bold indicate optimal graphs found with such a distance; only such graphs were used for calculating the cycle erasure threshold p_E^0, see Figs. 4.10 and 4.12. Percolation transition critical point p_c on the infinite hyperbolic graph $\mathcal{H}_{f,d}$ (same as the giant cluster transition) was calculated using all graphs in the corresponding family, with the exception of graphs whose distances are shown in gray. Graphs families $\{4, 7\}$ and $\{5, 6\}$ had less than three optimal graphs, so none of their threshold were calculated.

4.2 Percolation Methods

To simulate percolation, we used a version of the Newman–Ziff (NZ) Monte Carlo algorithm [46]. This is a Monte Carlo type method which creates a canonical ensemble of edges and randomly orders them. The graph is initialized to be empty, all edges closed. A random edge is chosen to be opened. All statistics are then updated. This is repeated until all edges are open. Adding a singe edge is computationally inexpensive, and so the computational complexity of adding all edges to the graph is of only order n.

The original version of the algorithm is meant for a single graph. This would make it very difficult to update the homology rank when a new edge is added. However, if we adapt the algorithm to run on both the graph, $\mathcal{G}$ and its dual, $\widetilde{\mathcal{G}}$ we can use equation 2.14 to keep track of the number of homologies.

This was done by closing an edge on $[\widetilde{\mathcal{G}}]_p$ when an edge is opened on $[\mathcal{G}]_p$. Practically closing an edge then updating statistics is computationally hard. Instead, we reversed the edge ensemble list and opened edges in $[\widetilde{\mathcal{G}}]_p$ in the reverse order of $[\mathcal{G}]_p$. The cluster sizes of both graphs were saved, then once a sweep through both graphs is completed the homology rank is updated for the entire set of points.

Another issue is our simulations calculate averages for a given number of open edges (canonical ensemble), but we need averages for a given p value (grand-canonical ensemble). This means we need to convert from one to the other. This can be done by using the binomial distribution to calculate the corresponding grand-canonical quantity,

$$A_p = \sum_{i=0}^{n} b_{i,p} A_i \tag{4.2a}$$

$$b_{x,p} = \binom{n}{x} p^x (1-p)^{n-x}, \tag{4.2b}$$

where A_p is the average over constant p and A_i is the average over constant open edge count, for some observable A. In order to speed up calculations we ignored very small $b_{x,p}$ values, cutting off any $b_{x,p}$ value which was over 100 standard deviations away from the mean, $|x - pn| < M\sqrt{np(1-p)}$, with $M = 10^2$. For each graph we ran 10^6 runs, saving the grand-canonical averages of observables for $10^3 + 1$ p values, with intervals of $\Delta p = 10^{-3}$, and three data runs were performed, so each percolation transition was calculated three separate times to obtain an independent estimate of the errors. The averaged observables calculated, all implicit functions of p, are: k, S_1, S_2, S_2/S_1, $\mathbb{P}_p(\operatorname{rank} H_1 > 0)$, $\operatorname{rank} H_1$, $|\mathcal{K}_0|$ and the corresponding values squared, where k is the number of clusters, S_i is the size of the ith largest cluster, $\mathbb{P}_p(\operatorname{rank} H_1 > 0)$ is the probability at least 1 homology is covered, the erasure probability, $\operatorname{rank} H_1$ is the number of homologies covered, and $|\mathcal{K}_0|$ is the size of the cluster connected to site 0.

4.2.1 Inflection Point Extrapolation

Inflection point extrapolation is a simple method we performed to find critical p values for a given finite graph, which are then used to find the threshold value for an infinite graph using finite size scaling methods described later. This method consists of finding the inflection point near the percolation transition, then finding the tangent line of this point. We then take the tangent line and extrapolate it to a particular y value, like $y = 0$, $y = 1$ or the inflection point itself. An example of this method can be seen

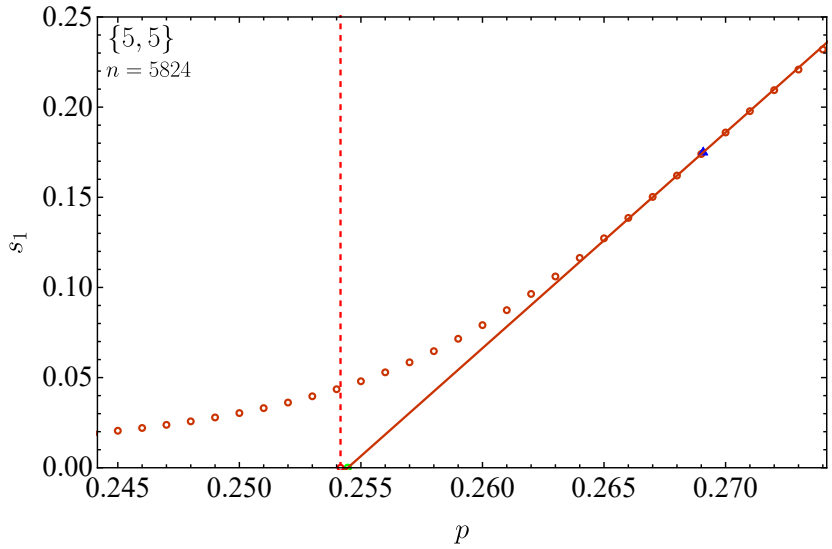

Figure 4.1: Example of an inflection point extrapolation fit. This plots the fractional size of the largest cluster, s_1, versus p. The red line is the tangent line to the inflection point, which is shown in blue. The extrapolation point is the intersection of this line with $s_1 = 0$, which is shown in green. The green point is then taken to be our critical p value for this finite graph.

in Fig. 4.1.

This method is justified in cases where the slope of the inflection point tends to infinity, and it also moves towards the extrapolation point. If it moves away from the extrapolation point we might have unexpected behavior. We use this method in 4 different cases: p_G, $p_c^{(S)}$, $p_E^{(0)}$, $p_E^{(I)}$, and $p_E^{(1)}$, as explained in future sections.

4.2.2 Finite Size Scaling

Finite size scaling is one of the many techniques where the data calculated in a finite-size system (a sequence of finite graphs in our case) is extrapolated to an infinite size. We did this by taking a set of paired critical values (n, p_n), where p_n is the critical p value found for the graph of size n. The method to determine the critical p value depends on which threshold is being calculated. The critical p values, p_n, for a finite

graph were obtained using inflection point extrapolation, as explained above, or where the p value such that the largest cluster is related to the graph size, $S_1 = |\mathcal{V}|^{2/3}$, which is explained in more detail later. These points are then extrapolated to the infinite size limit giving us the threshold value (∞, p_c). This extrapolation was done by performing a fit of the form

$$p(x) = \sum_{i=0}^{a} C_i (\frac{1}{x^\gamma})^i, \tag{4.3}$$

where C_i are fit parameters, a and γ are constants and the infinite limit threshold value is C_0. The value for γ was kept at a constant 1/3 or 2/3, and a was chosen to minimize the fit's residue without over fitting.

The value for γ comes from the critical exponents for hyperbolic graphs. Hyperbolic graph families can be viewed as having infinite dimension, so they fall into the mean field theory regime with dimension greater than 6. The corresponding finite-size scaling can be conveniently recast to the system size, V, as an independent parameter. Namely, we consider a D-dimensional lattice, with $D > D_{\text{critical}} = 6$. This means near the percolation threshold the correlation function, ξ, and system size, V, relate to each other since the cut off for the correlation function is L. This gives us

$$V \propto L^6 \sim \xi^6 \propto |p - p_c|^{-6\nu} \implies |p - p_c| \propto V^{-1/3}, \tag{4.4}$$

where we have taken, the mean-field value for the correlation length exponent, $\nu = 1/2$ in high dimension regime. The largest cluster size, S_1, also relates to the correlation function using the fractal dimension, d_f,

$$S_1 \propto \xi^{d_f} \propto V^{d_f/6} \propto V^{2/3}. \tag{4.5}$$

These two relations justify our use for $\gamma = 1/3$ when performing finite size scaling, along

with one of the finite size scaling methods described later. These relations also agree with the form of critical scaling for random graph found in Ref. [29].

4.3 Percolation and Erasure Threshold Results

Tabs. 4.2 and 4.3 show summaries of the final calculated percolation thresholds and 4.4 shows the erasure thresholds. We found three different transition points p_c, p_G and p_E^0; p_c was calculated using 2 different methods, labeled as $p_c^{(2/3)}$ and $p_c^{(C)}$, and p_E^0 was calculated using 5 different methods, labeled as $p_E^{(C)}$, $p_E^{(\mathrm{shift})}$, $p_E^{(1)}$, $p_E^{(I)}$, $p_E^{(0)}$. Later sections will go more in depth about each calculation.

4.3.1 Results for p_c

Percolation Threshold Transition p values

$\{f,d\}$	$p_c^{(I)}$	$p_c^{(2/3)}$	$n_c^{(2/3)}$	$a_c^{(2/3)}$	$p_c^{(C)}$	$n_c^{(C)}$	$a_c^{(C)}$	$p_c^{(\mathrm{shift})}$	$n_c^{(\mathrm{shift})}$	B_c
{3,7}	0.1993505(7)	0.200(1)	0.649	2	0.2039(2)	22.75	4	0.2039(2)	22.75	0.081(5)
{7,3}	0.5305246(7)	0.532(1)	1.48	2	0.5369(3)	21.25	2	0.5355(3)	16.58	0.087(2)
{3,8}	0.1601555(7)	0.160(3)	-0.0518	3	0.16207(5)	38.29	9	0.16210(5)	38.89	0.26(1)
{8,3}	0.5136441(7)	0.514(2)	0.178	3	0.5187(2)	25.28	3	0.5188(2)	25.78	0.32(3)
{4,4}	0.5	0.4893(3)	-35.67	3	0.500011(6)	1.22222	4	0.50010(2)	5.	0.003(1)
{4,5}	0.2689195(7)	0.2693(5)	0.761	2	0.27010(3)	39.348	6	0.27007(4)	28.762	0.306(8)
{5,4}	0.3512228(7)	0.3518(6)	0.962	2	0.35253(3)	43.571	6	0.35249(3)	42.238	0.18(9)
{4,6}	0.20714787(8)	0.2076(2)	2.261	1	0.2077(1)	5.521	4	0.2077(1)	5.521	-0.08(3)
{6,4}	0.3389049(7)	0.3396(1)	6.951	1	0.33971(9)	8.9455	3	0.33966(8)	9.4387	0.14(4)
{7,4}	0.33526580(8)	0.3359(6)	1.057	2	0.33680(8)	19.177	6	0.3361(4)	2.085	0.24(8)
{5,5}	0.25416087(8)	0.2545(7)	0.4845	2	0.25489(3)	24.304	6	0.25492(3)	25.304	0.88(6)
{6,5}	0.25109739(8)	0.251(1)	-0.0974	2	0.25227(8)	14.658	4	0.25215(9)	11.696	0.053(5)
{r,5}	0.25	0.2500(2)	0.	2	0.25012(1)	12.	4	-	-	-

Table 4.2: Critical p_c values found for graph families characterized by Schläfli symbols $\{f,d\}$, where $f = r$ stands for random graphs of degree d. Here $p_c^{(I)}$ is the percolation threshold (using invasion percolation data from Ref. [45], or exact values where known), $p_c^{(2/3)}$ and $p_c^{(C)}$ are the traditional percolation thresholds using random-graph-like cluster size scaling (see Fig. 4.3) and the cluster-ratio (see Figs. 4.4 and 4.5), respectively. Numbers in the parenthesis indicate the standard deviation σ in the units of the last significant digit, so that, e.g., $0.14(4) \equiv 0.14 \pm 0.04$. Values of $n_c \equiv (p_c - p_c^{(I)})/\sigma$ give the "number of sigmas" from the deviation of the corresponding critical value found from the invasion percolation, or exact threshold value if available. Numbers in columns labeled a give the degrees of the polynomials used to interpolate the data; polynomials of the same degrees were used to obtain $p_c^{(C)}$ and $p_c^{(\mathrm{shift})}$.

We compute p_c to verify our simulation results and we use different methods and compare them to make sure these methods work well and agree with known values. We have used several finite-size scaling techniques to extract the location of the percolation thresholds which coincides with the giant-cluster threshold, see Theorem 1.3 in Ref. [3]. All techniques, besides the cluster-size ratio technique [42, 12] in the case of hyperbolic graphs and the giant-cluster threshold, give transition points in a reasonable agreement with the values expected from invasion percolation simulations in Ref. [45]. For hyperbolic graphs, we found the most accurate values of p_c are found using the technique based on the expectation of cluster size scaling similar to that for random graphs [38, 29], $S_1 \propto n^{2/3}$ near p_c, with the critical region of width $|p - p_c| \sim n^{-1/3}$. Respectively, when interpolated values of p such that the expected size of the largest cluster satisfies $S_1(p) = \omega n^{2/3}$ are plotted for $\omega \in \{1/4, 1/2, 1\}$ as a function of $x \equiv n^{-1/3}$, the data for graphs with different n fit nicely, and can be extrapolated to $x = 0$ (infinite graph size) using polynomial fits, see Fig. 4.3. Notice that while this technique works well for hyperbolic graphs and for random graphs, in our simulations it failed dramatically for the euclidean $\{4, 4\}$ graph family, as can be seen from the corresponding value of $p_c^{(2/3)}$ in Tab. 4.2.

The first method to calculate the percolation threshold is meant specifically for random and hyperbolic graphs. We denoted this as $p_c^{(2/3)}$. The second method is the cluster-ratio method. This method has been proved to work for metric graphs [42], and is commonly used as a numerical method for other types of graphs. We denote this as $p_c^{(C)}$. Additionally we introduce a shift into the cluster-ratio method to obtain a third p_c estimate labeled as $p_c^{(\text{shift})}$

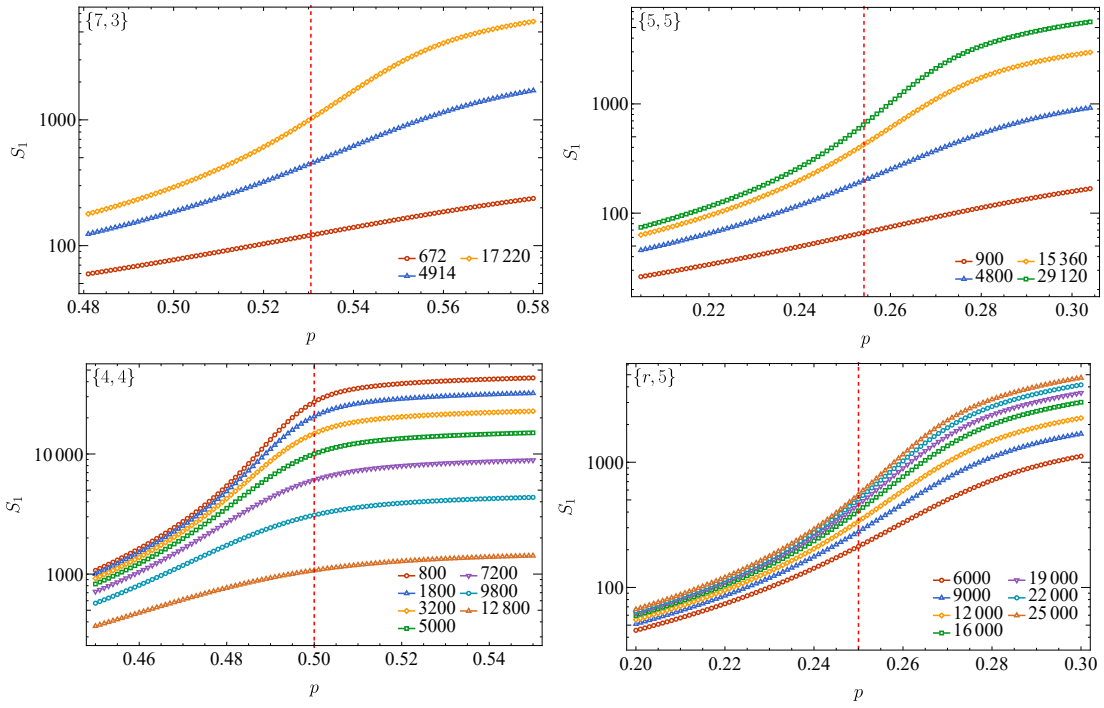

Figure 4.2: The size of the largest cluster versus p as a log-linear plot. The dashed red lines represents $p_c^{(I)}$, and the graphs are labeled by n. The error bars are too small to see. These are for illustration purposes and samples of the data is used elsewhere.

The first method is taken from Ref. [29] and comes from equation 4.5. It has been derived for the random and larger hypercubic graphs. Hyperbolic graphs have similar properties to random graphs, specifically they are both expander graphs. In the absence of uniqueness, there are multiple percolation clusters on an infinite graph. For a finite graph these are connected, but in a random fashion, which explains the analogy with the random graphs which asymptotically behave like trees.

This method uses finite size scaling on critical p values within the scaling window for each graph, which is used to find the critical p value in the infinite graph limit, $p_c^{(2/3)}$. The critical values are defined to be the p value such that $S_1 = \omega|\mathcal{V}|^{2/3}$, where S_1 is the size of the largest cluster. We show in Fig. 4.3 multiple values for ω to show the stability of this method.

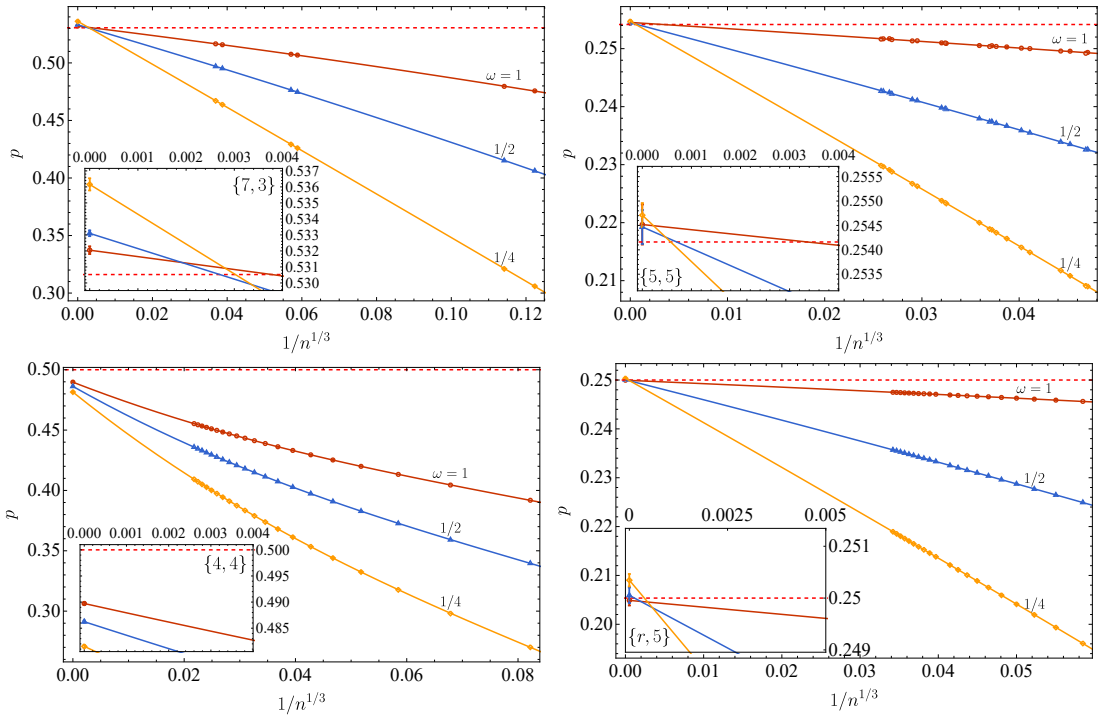

Figure 4.3: Finite size scaling of the critical p values to find $p_c^{(2/3)}$, for $\{f, d\}$ graph families as indicated in the captions. The p values are solutions to the equation $S_1 = \omega|\mathcal{V}|^{2/3}$, where S_1 is the largest cluster for a given p value. The dashed red line is at $p_c^{(I)}$. The lines intersect close to the expected percolation transition point, except for the $\{4, 4\}$ graph as expected, since this graph is not an expander graph.

The second method, the cluster-ratio method, is a more standard way to find the percolation threshold [42, 12, 39]. This method has been proved for metric graphs, and numerically shown to work for other graph families [42].

We achieved this by doing a simultaneous multi-plot fit of all the graphs of the form $y_c + \sum_{i=1}^{a} A_n^{(i)}(x - x_c)^i$ where each $A_n^{(i)}$ is different for each graph, but x_c and y_c are kept the same across all the graphs. The polynomial degree a was chosen using the same criteria as for the finite size scaling method previously described. Only data near the crossing point was used. This gives the crossing point of the collection of graphs to be (x_c, y_c), and therefore $p_c^{(C)} = x_c$ is the infinite graph critical value. Plots for S_2/S_1, the ratio between the largest and second largest clusters, can be seen in Fig. 4.4, while

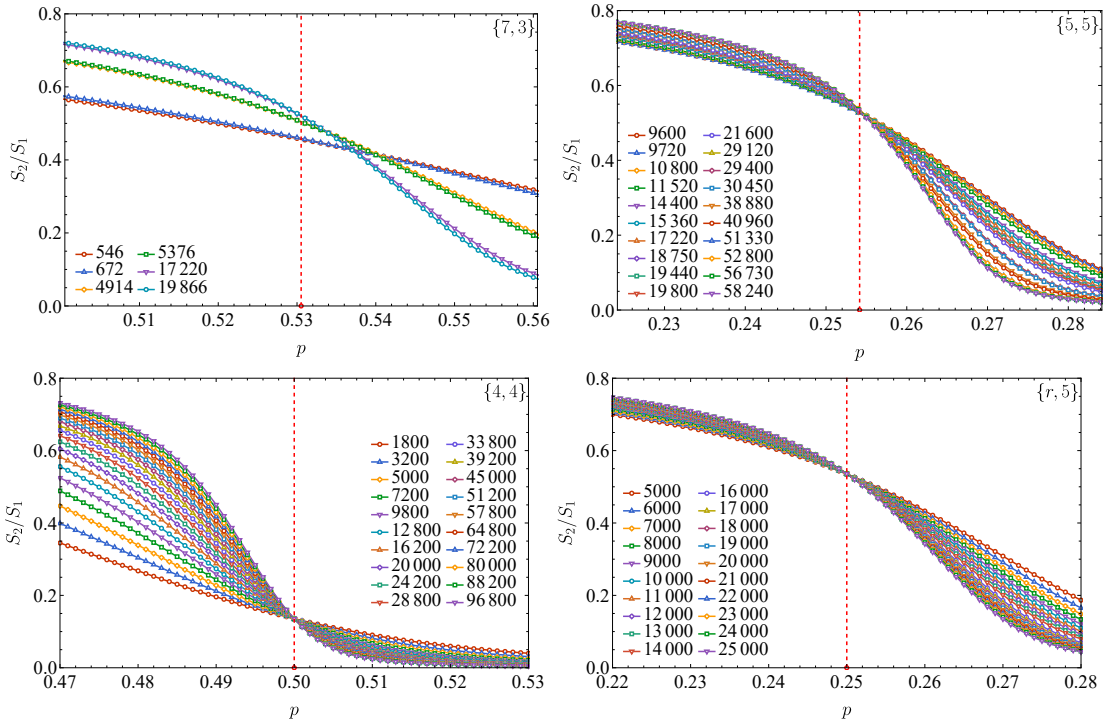

Figure 4.4: Plots of S_2/S_1, ratio between the largest and second largest cluster sizes, verses p. The red dashed is at $p_c^{(I)}$, the expected percolation threshold, and the graphs use n, the edge count, as labels. The error bars are too small to see. Look at Fig. 4.5 for more details near the crossing point.

a zoomed in view at the crossing point can be seen in Fig. 4.5.

Looking at Fig. 4.5, a clear difference can be seen between the hyperbolic graphs and the non-hyperbolic graphs. Numerically, there is a larger difference between the expected result shown by the dashed red line and our calculated result. The convergence near the crossing point is poor for the hyperbolic graphs, but it is much better for non-hyperbolic graphs. We conclude that even though the method of finding the crossing point of S_2/S_1 works in many cases, it fails for hyperbolic graphs and its use should be limited to lattices in finite dimensions and to random graphs, as it was derived for graphs where usual critical scaling works [42]. The difference between the expected result

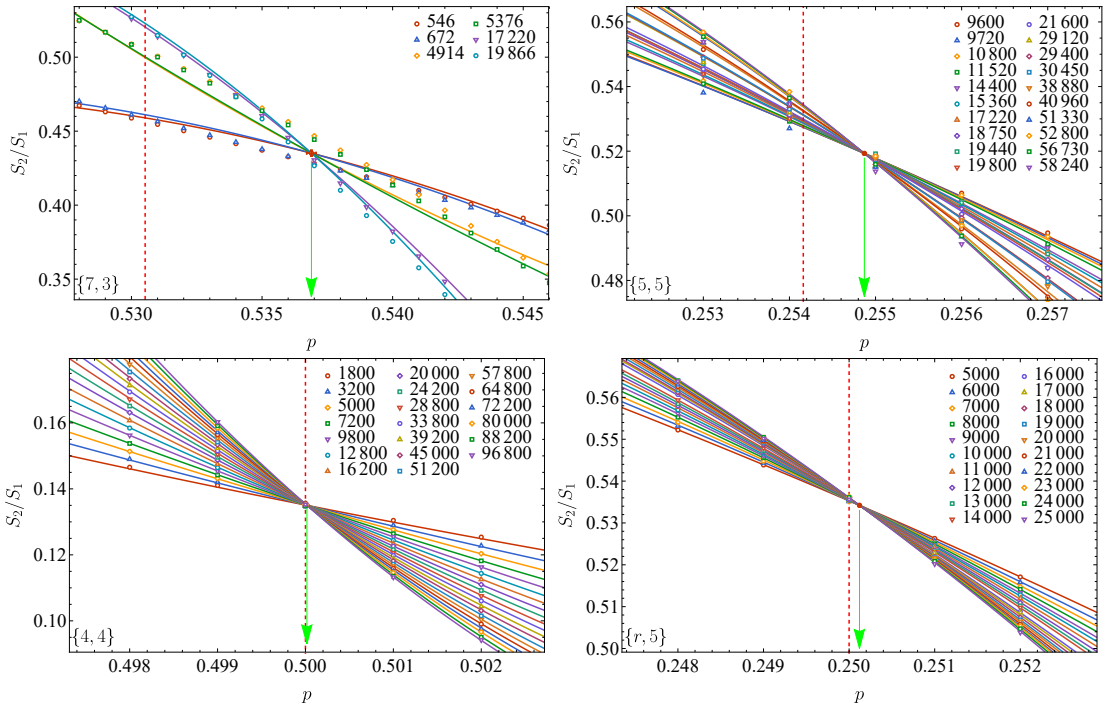

Figure 4.5: Plot of the crossing point of S_2/S_1, the ratio between the largest and second largest cluster sizes, used to calculate $p_c^{(C)}$. The red point is the estimated crossing point with error bars. The dashed red line is at $p_c^{(I)}$, the expected percolation threshold value, and the labels are of n, the edge count. The lines are the fit lines used to find $p_c^{(C)}$. It is clear the crossing point of the hyperbolic graphs $\{7,3\}$ and $\{5,5\}$ are significantly farther away from $p_c^{(I)}$ than the euclidean $\{4,4\}$ and random $\{r,5\}$ graphs.

and calculated result for the $\{r,5\}$ graph can easily be explained through the large gap between p values. However, this same explanation is not true for the hyperbolic graphs.

When looking at the crossing points in Fig. 4.5, the hyperbolic graphs have much larger deviations in the positions of their curves. This difference can be accounted for due to their differences in the ratio $\ln n/d$, where d is the distance of the graph. New plots with a shift factor to account for this difference are shown in Fig. 4.6. This shift was calculated through adding a term $B \ln n/d$ to the fit of S_2/S_1, where B is a fitting parameter which is constant for all graphs. These B values are listed in Tab. 4.2, along with the new critical percolation values of $p_c^{(\text{shift})}$.

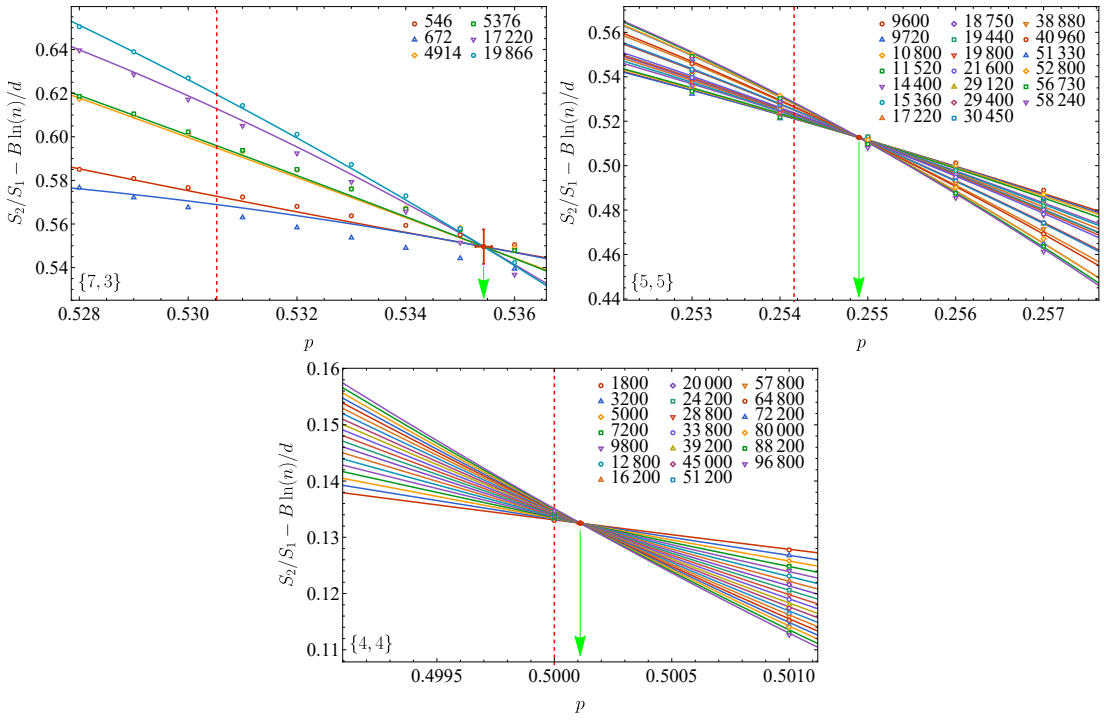

Figure 4.6: Plot of the crossing point of S_2/S_1, the ratio between the largest and second largest cluster sizes, with a finite size shift factor used to calculate $p_c^{(\text{shift})}$, where d is the distance of the graph. The red point is the estimated crossing point with error bars. The dashed red line is at $p_c^{(I)}$, the expected percolation threshold value, and the labels are of n, the edge count. The lines are the fit lines used to find $p_c^{(\text{shift})}$. It is clear the crossing point of the hyperbolic graphs $\{7, 3\}$ and $\{5, 5\}$ are significantly farther away from $p_c^{(I)}$ than the euclidean $\{4, 4\}$ graph.

Overall, the final estimated percolation threshold value does not change. The only graph which had a significant difference between $p_c^{(C)}$ and $p_c^{(\text{shift})}$ is the $\{7, 4\}$ graph family. However, this is mainly due to the increased value in the error, not in a significant shift in the crossing point. For the hyperbolic graphs, the shifted plots show a much better convergence near the crossing point, but it is still many sigmas away from the expected percolation threshold. Taking into account Figs. 4.5 and 4.6 along with the results for $p_c^{(C)}$ and $p_c^{(\text{shift})}$ shown in Tab. 4.2, we have strong numerical evidence the cluster-ratio method does not give p_c for hyperbolic graph families, with the exception of random graphs which have substantially fewer short cycles.

4.3.2 Results for p_G

Giant Cluster Threshold Transition p value

$\{f,d\}$	$p_c^{(I)}$	p_G	n_G	a_G
{3,7}	0.1993505(7)	0.2026(3)	10.83	2
{7,3}	0.5305246(7)	0.5350(4)	11.19	2
{3,8}	0.1601555(7)	0.162(2)	0.922	2
{8,3}	0.5136441(7)	0.515(2)	0.678	1
{4,4}	0.5	0.4919(2)	-40.5	5
{4,5}	0.2689195(7)	0.2704(2)	7.402	2
{5,4}	0.3512228(7)	0.3533(4)	5.193	2
{4,6}	0.20714787(8)	0.2084(1)	12.52	1
{6,4}	0.3389049(7)	0.3401(3)	3.984	2
{7,4}	0.33526580(8)	0.3370(4)	4.335	3
{5,5}	0.25416087(8)	0.2553(6)	1.899	2
{6,5}	0.25109739(8)	0.253(1)	1.9	2
{r,5}	0.25	0.2514(1)	13.5	2

Table 4.3: Giant cluster threshold, p_G, values found for graph families characterized by Schläfli symbols $\{f,d\}$, where $f = r$ stands for random graphs of degree d. Here $p_c^{(I)}$ is the percolation threshold (using invasion percolation data from Ref. [45], or exact values where known), and p_G is the giant cluster threshold (see Fig. 4.7). Numbers in the parenthesis indicate the standard deviation σ in the units of the last significant digit, so that, e.g., $0.14(4) \equiv 0.14 \pm 0.04$. Values of $n_G \equiv (p_G - p_c^{(I)})/\sigma$ give the "number of sigmas" from the deviation of the corresponding critical value found from the invasion percolation, or exact threshold value if available. Numbers in columns labeled a_G give the degrees of the polynomials used to interpolate the data.

To find the giant cluster threshold, p_G, we used finite size scaling, where the p_n values are found using inflection point extrapolation of the fractional size of the largest cluster, $s_1 = S_1/|\mathcal{V}|$, to $s_1 = 0$. Unfortunately, this kind of extrapolation proved unreliable for both hyperbolic and random graphs, see Fig. 4.7.

Indeed, for large graphs without a boundary, we expect this quantity to behave similarly to $\theta_v(p)$, the probability that vertex v is in an infinite cluster. For hyperbolic and random graphs, where the mean-field scaling $\theta_v(p) \propto (p - p_c)^\beta$, with the order parameter exponent $\beta = 1$ applies, the position of the inflection point is rather sensitive to the graph size and other details.

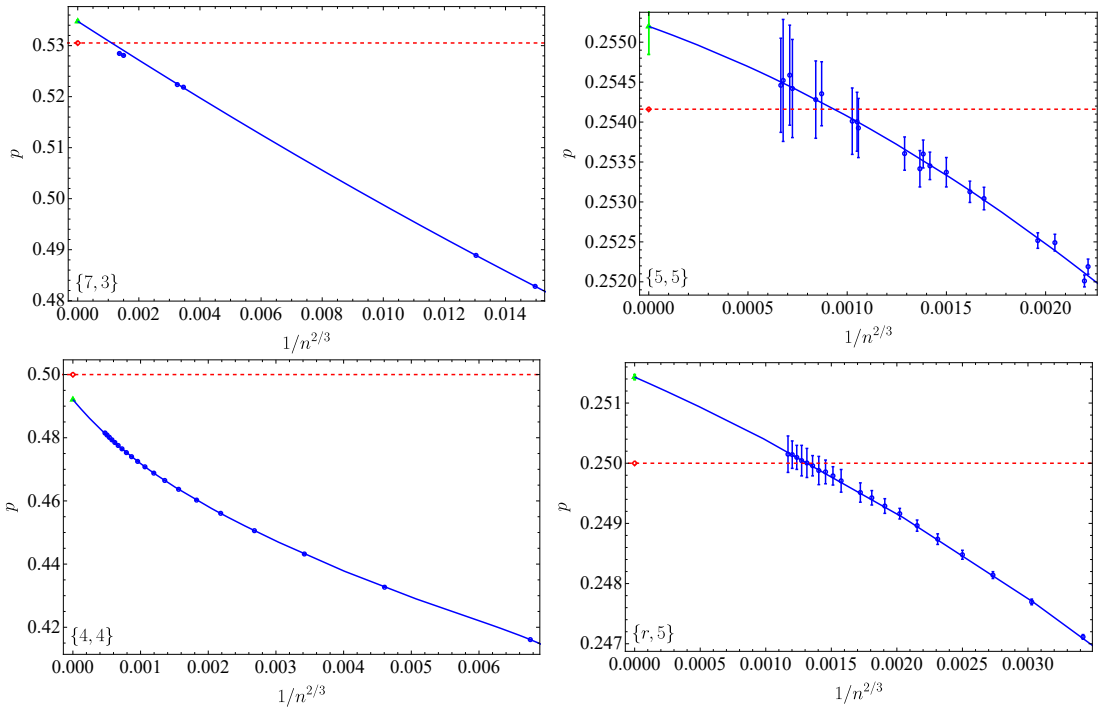

Figure 4.7: Finite size scaling fits to find the giant cluster threshold, p_G. Each p value is found by using inflection point extrapolation of s_1, the fractional size of the largest cluster. These values are scaled to an infinite size graph shown by the green point. The dashed red line is at $p_c^{(I)}$, the expected percolation threshold value.

On the other hand, for the square-lattice tori of finite size, the plots of $s_1(p)$ have positive curvature for $p \lesssim p_c$, which changes over to negative curvature characteristic of $\theta_v(p)$ with the critical exponent $\beta < 1$. The inflection point is indeed expected to remain inside the critical region, whose width goes to zero with increasing dimension L. Our results and scaling fits can be seen in Fig. 4.7 and Tab. 4.3.

4.3.3 Results for p_E^0

A de-facto standard way for estimating the erasure threshold p_E^0 is the crossing point method. The method is based on the expectation that the block error probability is asymptotically zero for any $p < p_E^0$ and is equal to one for $p > p_E^0$, with the crossover

Erasure Threshold Transition p values

$\{f,d\}$	$p_c^{(I)}$	$p_E^{(C)}$	$n_E^{(C)}$	$a_E^{(C)}$	$p_E^{(\mathrm{shift})}$	$n_E^{(\mathrm{shift})}$	B_E	$p_E^{(1)}$	$n_E^{(1)}$	$a_E^{(1)}$	$p_E^{(I)}$	$n_E^{(I)}$	$a_E^{(I)}$	$p_E^{(0)}$	$n_E^{(0)}$	$a_E^{(0)}$	$1/m$	a_m
{3,7}	0.1993505(7)	0.1941(2)	-26.25	6	0.19318(9)	-68.56	0.081(5)	0.196(1)	-3.35	1	0.200(2)	0.162	1	0.198(8)	-0.169	1	-0.006(9)	1
{7,3}	0.5305246(7)	0.52109(8)	-117.93	4	0.52042(5)	-202.07	0.087(2)	0.5274(5)	-6.249	1	0.52793(9)	-13.123	1	0.5229(4)	-19.06	1	0.0043(6)	1
{3,8}	0.1601555(7)	0.1519(4)	-20.64	7	0.1524(1)	-77.55	0.26(1)	0.1563(8)	-4.819	1	0.1597(6)	-1.155	1	0.156(2)	-2.08	1	-0.001(2)	1
{8,3}	0.5136441(7)	0.5032(2)	-52.22	6	0.5026(1)	-110.4	0.32(3)	0.5122(7)	-2.063	2	0.5107(1)	-9.48	1	0.505(4)	-2.16	2	0.006(3)	2
{4,4}	0.5	0.500004(6)	2.	6	0.499992(6)	-1.33333	0.003(1)	0.4997(1)	-3.	3	0.5006(1)	2.	3	0.5009(1)	9.	3	-0.0012(3)	3
{4,5}	0.2689195(7)	0.2581(2)	-54.1	5	0.2547(2)	-71.1	0.306(8)	0.2658(4)	-7.799	1	0.2664(3)	-4.199	1	0.261(2)	-3.96	1	0.004(2)	1
{5,4}	0.3512228(7)	0.3415(4)	-24.31	2	0.3412(4)	-25.06	0.18(9)	0.3498(7)	-2.033	2	0.3490(2)	-5.557	1	0.343(4)	-2.06	2	0.006(3)	2
{4,6}	0.20714787(8)	0.19564(4)	-287.7	3	0.1949(3)	-40.83	-0.08(3)	0.203(1)	-4.15	1	0.20455(1)	-37.541	1	0.19824(6)	-148.46	1	0.0050(7)	1
{6,4}	0.3389049(7)	0.3272(4)	-29.26	2	0.3275(3)	-38.02	0.14(4)	0.336(1)	-2.9	2	0.334(1)	-2.45	2	0.333(4)	-1.48	1	0.014(3)	2
{7,4}	0.33526580(8)	0.3200(2)	-76.33	10	0.323(1)	-12.3	0.24(8)	0.3338(5)	-2.932	2	0.3321(4)	-4.207	2	0.323(1)	-12.3	2	0.011(1)	2
{5,5}	0.25416087(8)	0.2437(4)	-26.15	5	0.2453(2)	-44.3	0.88(6)	0.2507(6)	-5.768	1	0.2515(1)	-6.652	1	0.245(1)	-9.16	1	0.005(1)	1
{6,5}	0.25109739(8)	0.2442(2)	-34.49	4	0.2429(1)	-81.97	0.053(5)	0.2478(6)	-5.496	1	0.24969(7)	-6.9869	1	0.2444(9)	-7.442	1	0.0035(3)	1

Table 4.4: The lower erasure threshold, p_E^0, values found for graph families characterized by Schläfli symbols $\{f,d\}$, where $f=r$ stands for random graphs of degree d. Here $p_c^{(I)}$ is the percolation threshold (using invasion percolation data from Ref. [45], or exact values where known). $p_E^{(C)}$ and $p_E^{(\mathrm{shift})}$ are the crossing point of the erasure probability, where the shift value has an extra shift of $B\ln n/d$ added to account for difference in the code rates (see Figs. 4.10 and 4.11). $p_E^{(1)}$, $p_E^{(I)}$ and $p_E^{(0)}$ were found using the tangent line of inflection point of the erasure probability; the intersection of this line with the erasure probability at 1, the inflection point, and 0 gave the three results respectively (see Fig. 4.12). The inverse slope, $1/m$, is the inverse of the slope at the inflection point of the erasure probability (see Fig. 4.13). Numbers in the parenthesis indicate the standard deviation σ in the units of the last significant digit, so that, e.g., $0.14(4)\equiv 0.14\pm 0.04$. Values of $n_E\equiv(p_E-p_c^{(I)})/\sigma$ give the "number of sigmas" from the deviation of the corresponding critical value found from the invasion percolation, or exact threshold value if available. Numbers in columns labeled a_E give the degrees of the polynomials used to interpolate the data; polynomials of the same degrees were used to obtain $p_E^{(C)}$ and $p_E^{(\mathrm{shift})}$.

region small for large codes. Respectively, when the erasure probability found numerically for several graphs is plotted as a function of p, the corresponding lines are expected to cross in a single point, which is identified as the pseudothreshold.

This works well for codes with power-law distance scaling. An example is shown in Fig. 4.10 of the $\{4,4\}$ graph, where the homological error probability (3.1) for several square lattice toric codes with parameters $[[2d^2,2,d]]$ and d ranging from 60 to 220 is plotted as a function of the open edge probability p. Visually, a beautiful crossing point close to $p_E^0=1/2$ is observed. To find the corresponding erasure pseudothreshold, the data was fitted collectively with polynomials of $\xi\equiv p-p^0$. In the same way the crossing point of S_2/S_1 is found above for the cluster-ratio method.

For the square-lattice graphs, using 6th degree polynomials, we obtained $p^0(\{4,4\})=$

0.500004 ± 0.000002, very close to the square lattice percolation threshold $p_c(\{4,4\}) = 1/2$, as expected from Refs. [50, 23] and Theorem 9. The corresponding linear terms A_{1n} (the derivative at the crossing point) have a power law $A_{1n} = bn^{\alpha}$ scaling (not shown), with the exponent $\alpha = 0.375 \pm 0.003$, consistent with the expectation of a sharp threshold in the large-n limit.

We used a similar technique to process the homological error probability data for hyperbolic graphs. A sample of the corresponding plots is also shown in the Fig. 4.10. These plots have two significant differences with the $\{4,4\}$ graphs. First, the crossing points are significantly below the percolation transitions indicated by the vertical dashed lines. Second, despite smaller scales, the convergence near the crossing points does not look as nice. Empirically, deviations in the position of the curves are associated with the differences in the ratio $\ln n/d$, cf. the bounds in Statements 4, 5 and Example 11. To reduce the corresponding errors in the calculation of the erasure thresholds we only used the optimal graphs, shown in Tab. 4.1 with the distance shown in bold.

Yet, using only the optimal graphs was not sufficient to completely eliminate the finite-size variation. Much better crossing points are obtained by introducing a vertical shift $B \ln n/d$, where B is an additional global fit parameter (see plots in Fig. 4.11), similar to how it was performed for the crossing point of S_2/S_1 in Fig. 4.6.

In comparison, the crossing point method does not work for measuring the location of the homological transition p_H^0, even though the variation between the graphs is not expected to matter that much here. Main reason for the difference is that the erasure rate (3.9) retains a finite slope in the infinite graph limit, which makes the crossing point analysis unreliable.

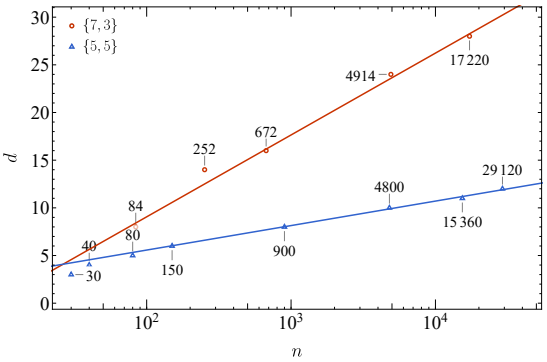

Figure 4.8: Homological distance $d \equiv d_Z$ associated with non-trivial cycles for optimal graphs in $\{7, 3\}$ and $\{5, 5\}$ families vs. the graph size n (number of edges) with the logarithmic scale. Numbers also indicate the graph sizes. Smaller relative distances $d/\ln n$ result in larger erasure probabilities in Figs. 4.10; this can be compensated to some extend by using the correction term as in plots in Fig. 4.11.

Numerical data indicates, as seen in Tab. 4.4, the erasure (pseudo)threshold is substantially below p_c for hyperbolic graphs with logarithmic distance scaling, with the variation of the ratio $\ln n/d$ having a significant effect on the quality of the crossing point. In contrast, for graphs from the $\{4, 4\}$ family where $d \propto n^{1/2}$, the cycle erasure (pseudo)threshold is very close to the bulk percolation threshold, as generally expected from Refs. [50, 23] and Theorem 9.

The next erasure threshold methods use the tangent line created from performing inflection point extrapolation, similar to how p_G was calculated. We looked at our erasure probability data and found the inflection point moved closer to $\mathbb{P}_p(\operatorname{rank} H_1 > 0) = 1$ as n increases. For each graph, the position of the inflection point and the corresponding slope were calculated from the polynomial fits to the data. Subsequently, we extrapolated to three different points: down to $\mathbb{P}_p(\operatorname{rank} H_1 > 0) = 0$, at the inflection point itself and up to $\mathbb{P}_p(\operatorname{rank} H_1 > 0) = 1$, each of which corresponds to $p_E^{(0)}$, $p_E^{(I)}$ and

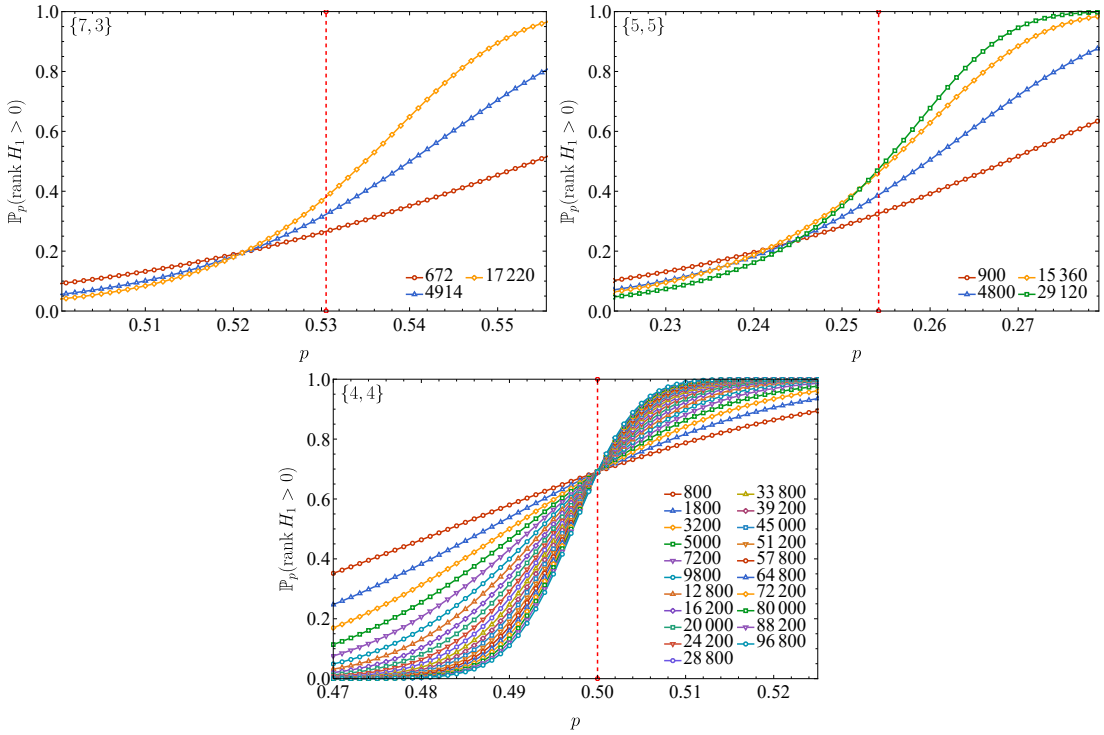

Figure 4.9: Example plots of $\mathbb{P}_p(\text{rank}\, H_1 > 0)$, the erasure probability, where the red dashed line is at $p_c^{(I)}$, the expected percolation threshold, and the labels are using n, the edge count. A zoomed in view near the crossing point can be seen in Fig. 4.10.

$p_E^{(1)}$ respectively. The finite size scaling fits can be seen in Fig. 4.12. We also calculated the slope at the inflection point and used finite size scaling to estimate the slope of the infinite sized graph, which can be seen in Fig. 4.13. The final results can be seen in Tab. 4.4.

These three p_E^0 values, along with the inverse slope, are not as good estimates for p_E^0 as the crossing point method, $p_E^{(C)}$. However, they can be used to justify the crossing point method and give further evidence $p_E^0 < p_c$ for the hyperbolic graphs. Looking at the results for the inverse slope, $1/m$, in Tab. 4.4 and Fig. 4.13, the square-lattice, $\{3, 7\}$ and $\{3, 8\}$ graph families have an inverse slope which approaches 0. In contrast to the other hyperbolic graphs, which the inverse slopes extrapolate to values

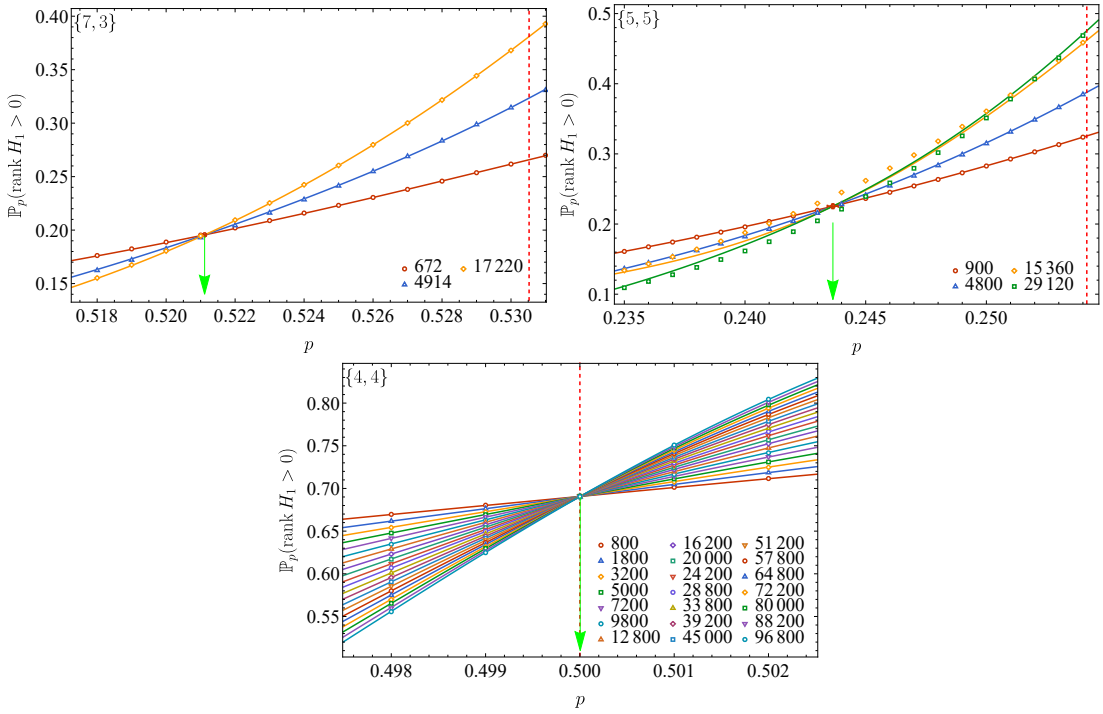

Figure 4.10: Plots showing the crossing point of the erasure data. The green arrow indicates the position of the crossing point found by the fit. The horizontal dashed line is at $p_c^{(I)}$, the expected percolation threshold, and n, the edge count, is being used has labels for each graph. The solid lines are the fitted lines for the data.

larger than 0.

Because of the slope being finite for hyperbolic graphs, we do not expect $p_E^{(1)}$ or $p_E^{(I)}$ to equal p_E^0. However, they do give a strong upper bound on p_E^0. The critical value $p_E^{(0)}$ does give a better estimate for p_E^0, but since the inflection point of $\mathbb{P}_p(\text{rank } H_1 > 0)$ moves upwards, this value is also an upper bound on p_E^0. We can see in Fig. 4.12 for the hyperbolic graphs $\{7,3\}$ and $\{5,5\}$, $p_E^{(1)}$ and $p_E^{(I)}$ agree with each other, while $p_E^{(0)}$ is significantly lower and all three are significantly lower than p_c. In contrast, the non-hyperbolic $\{4,4\}$ family, all three agree with each other and with p_c. Looking at final critical values in Tab. 4.4 for the hyperbolic graphs we have shown numerically,

$$p_E^0 \simeq p_E^{(shift)} \lesssim p_E^{(0)} < p_E^{(I)} \simeq p_E^{(1)} \lesssim p_c, \tag{4.6}$$

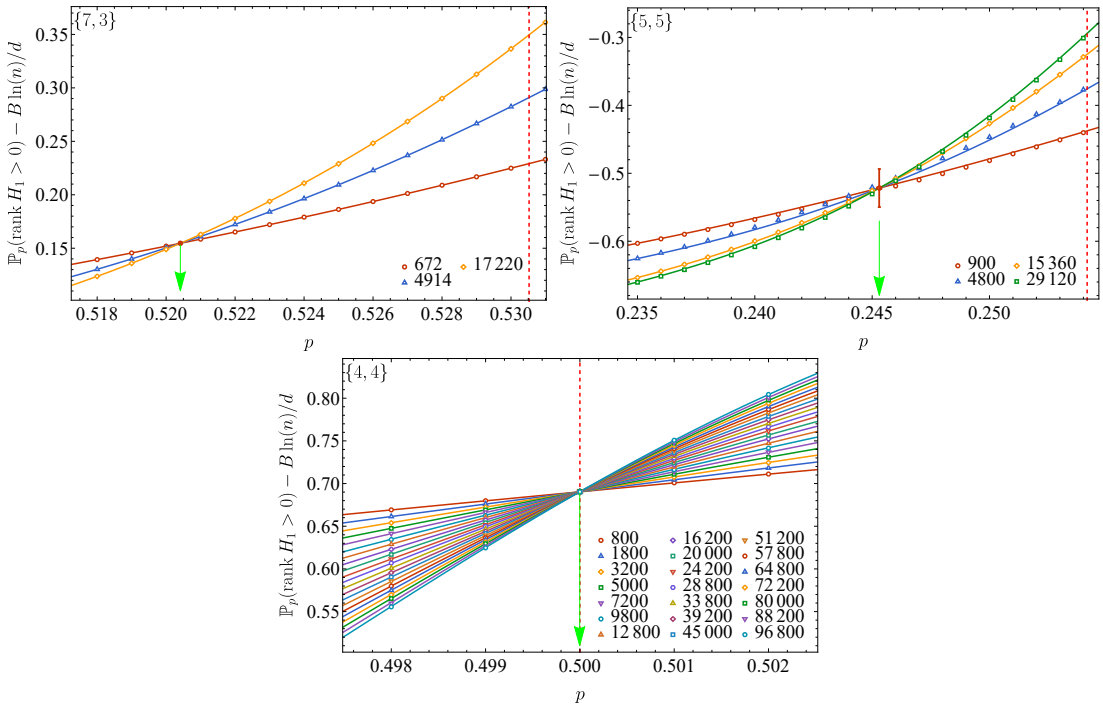

Figure 4.11: Plots showing the crossing point of the erasure probability. The green arrow indicates the position of the crossing point found by the fit. The red horizontal dashed line is at $p_c^{(I)}$, the expected percolation threshold. The solid lines are the fitted lines for the data. The plots for the hyperbolic graphs, as compared to those seen in Fig. 4.10, have a much better convergence to the crossing point. This crossing point is still significantly smaller than the expected p_c value.

and for the euclidean $\{4, 4\}$ family all erasure critical values are at p_c. These results give strong numerical evidence $p_E^0 < p_c$ for hyperbolic graphs, while $p_E^0 = p_c$ for euclidean graphs, agreeing with Theorems 6 and 9 and Example 11.

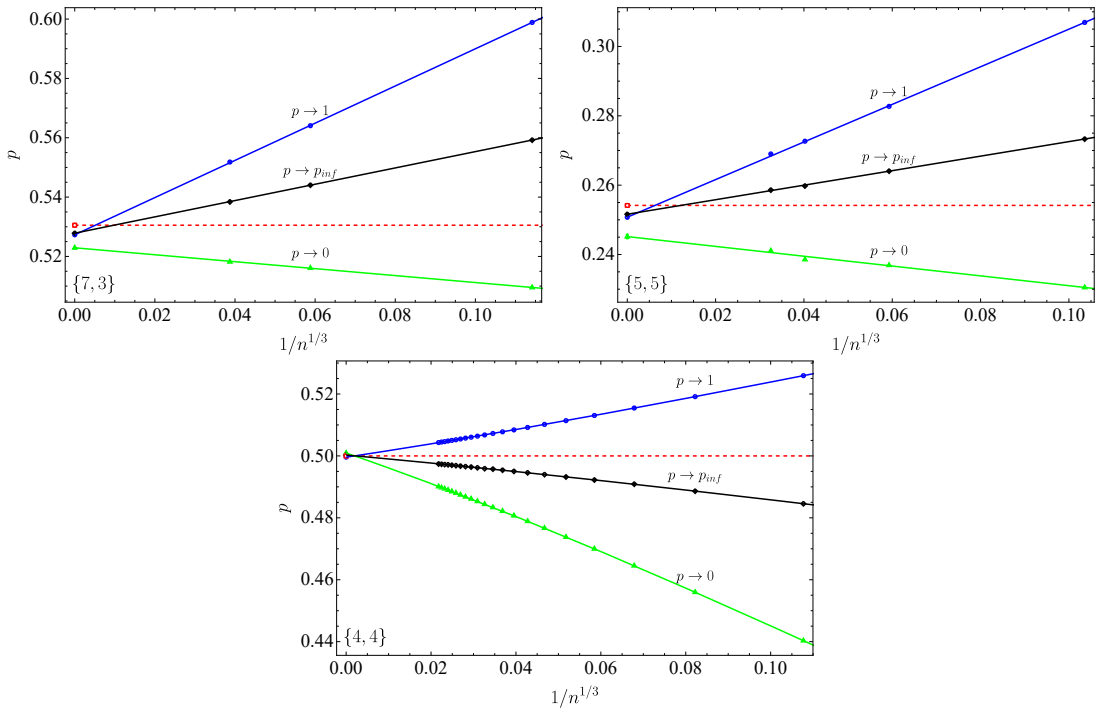

Figure 4.12: Shows the finite size scaling used to find $p_E^{(1)}$, $p_E^{(I)}$ and $p_E^{(0)}$. Each p value is found by taking the tangent line of the inflection point, and then finding the p value such that the erasure probability is 1, p_{inf} or 0, where p_{inf} is the inflection point itself. These values are fitted and scaled to find the p value for an infinite graph. The dashed red line is at $p_c^{(I)}$. For the hyperbolic graphs $\{7, 3\}$ and $\{5, 5\}$, $p_E^{(1)}$ and $p_E(I)$ agree with each other, while $p_E^{(0)}$ is significantly lower and all three are significantly lower than p_c, but for the non-hyperbolic graph, $\{4, 4\}$, all three agree with each other and with p_c.

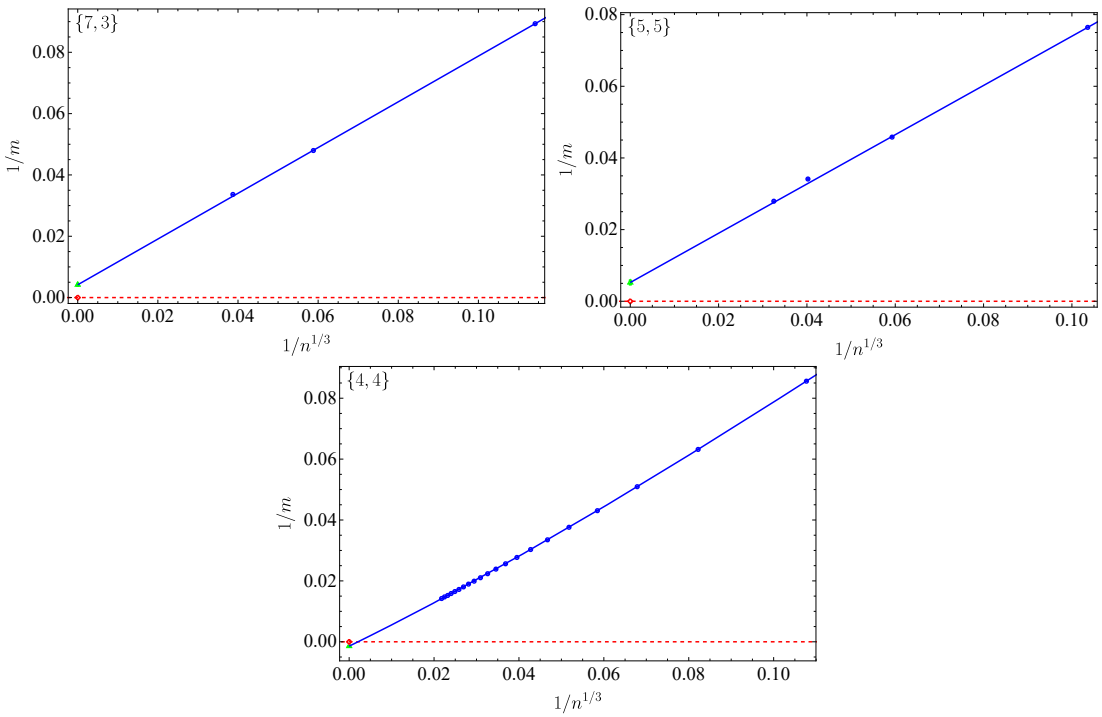

Figure 4.13: Shows the finite size scaling fits used to find the inverse slope at the inflection point in the infinite graph limit. Each slope value is calculated for each graph at the inflection point of the erasure probability. The inverse of this slope is taken and they are scaled to find the inverse slope for an infinite graph which is shown by the green point. The dashed red line is at 0, where we would expect the inverse of the slope to equal if the slope approached infinity.

Chapter 5

Conclusions

In this work we focused on critical points associated with homology-changing percolation transitions in a sequence of finite graphs weakly convergent to an infinite graph $\mathcal{H}$, a covering graph of the graphs in the sequence. We presented numerical evidence to support our stated theorems along with evidence for conjectures related to graphs with logarithmic distance scaling. Mainly we show the erasure threshold is less than the percolation threshold for graphs with logarithmic distance scaling, where the lower erasure threshold is the largest p value such that no homology is covered and the percolation threshold is the smallest p value such that an infinite cluster exists. We also present multiple methods which attempt to find the percolation threshold, and we comment on their reliability for hyberbolic graphs.

The position of the homological 1-cycle erasure threshold p_E^0 is governed by the scaling of the homological distance d with $\ln n$, where d is the size of a smallest non-trivial cycle and n is the graph size (number of edges). Generally, $p_E^0 \leq p_c(\mathcal{H})$, where the equality is reached for superlogarithmic distance scaling, while $p_E^0 = 0$ is expected

for sublogarithmic distance scaling. In the case of logarithmic distance scaling where the quantity $d/\ln n$ remains bounded away from 0 and from infinity, the cycle erasure threshold p_E^0 remains strictly positive as long as $\mathcal{H}$ is a bounded-degree graph, and we expect p_E^0 to be strictly below p_c. A strict proof of this is not given, but numerical evidence shows it to hold in the case of hyperbolic graphs.

For an amenable graph $\mathcal{H}$ with a finite isoperimetric dimension, an easy upper bound on the distance can be constructed by considering a ball with the radius equal to the injectivity radius, giving a power-law scaling of the distance with n. Generically, we expect that a sequence of covering maps with superlogarithmic distance scaling can be constructed when such a graph is quasitransitive, resulting in $p_E^0 = p_c(\mathcal{H})$. In particular, this is the case for any periodic lattice in dimension $D > 1$, since covering maps can be constructed by using periodic boundary conditions along each axis.

On the other hand, logarithmic scaling of the distance is the most one can expect when $\mathcal{H}$ is non-amenable. For such a graph the uniqueness threshold is expected [27] to be strictly higher than the percolation threshold, $\Delta p \equiv p_u(\mathcal{H}) - p_c(\mathcal{H}) > 0$, which gives a non-trivial upper bound for the asymptotic rate, $R \leq \Delta p$, where $R > 0$ corresponds to an extensive scaling of the homology rank associated with non-trivial 1-cycles. For any graph sequence with $R > 0$, we also introduced a pair of homological thresholds p_H^0 and p_H^1, associated with the points where asymptotic erasure rate (3.9) deviates from the values at $p = 0$ and $p = 1$, respectively. Generally, $p_H^0 \geq p_c$; for planar transitive graphs we proved $p_H^0 = p_c(\mathcal{H})$ and $p_H^1 = p_u(\mathcal{H})$. We conjecture this to be the case more generally.

Numerically we verified our results and gave threshold results for the case of

hyperbolic graphs, which have logarithmic distance scaling. First we calculated the p_c using two main methods. The first uses the crossing point of the cluster-ratio, which has been proven to work for metric graph, and is generally accepted to work for most finite size graph families. However, we show for hyperbolic graphs, this method works poorly. We verify this method works for the toric and random graph families. However, we also presented an alternative method to calculate p_c which is reliable for hyperbolic graphs, but it fails for the toric graphs. This method performs finite size scaling which extrapolates the p value on the finite graph such that the largest cluster, S_1 follows the relation $S_1 = |\mathcal{V}|^{2/3}$. This method gives good performance and agrees with the expected p_c value for hyperbolic graphs and random graphs since they are both expander graphs, but does fail for the square-lattice graphs.

We also calculated a pseudo-erasure threshold p_E^0. This was done by finding the crossing point of the erasure probability. We also performned finite size scaling of the inflection point tangent line. Our numerics showed strong evidence for hyperbolic graphs $p_E^0 < p_c$, but for the square-lattice and random graphs $p_E^0 = p_c$. We have proofs for the second result, but not for the first.

In order to obtain good numerics on hyperbolic graphs we needed to create hyperbolic CSS codes and their corresponding graphs. These graphs are non-trival to make. We found graphs of various hyperbolic graph families with graph sizes up to $\sim 10^5$ edges.

A number of open questions remain. First, related to the sequences of finite graphs both weakly convergent to an infinite graph $\mathcal{H}$, and covered by $\mathcal{H}$. What are the properties of $\mathcal{H}$ necessary for such a sequence to exist, in particular, is it necessary that

$\mathcal{H}$ be quasi-transitive? Second, is it true that with a logarithmic distance scaling, the strict inequality holds $p_E^0 < p_c(\mathcal{H})$? We have shown numerical evidence it is true, but to what extent, as indicated by Example 11 and numerics?

An important open question is to what extent present results can be extended to other models, in particular, Ising and, more generally, q-state Potts model on various graphs. Indeed, successful decoding probability in qubit quantum LDPC codes can be mapped to ratios of partition functions of associated random-bond Ising models [17, 37, 32]. In the clean (no-disorder) limit, these can be rewritten in terms of Fortuin-Kasteleyn (FK) random-cluster models. For such a model with $q \geq 1$, Hutchcroft [30] has recently proved the exponential decay of cluster size distribution in the subscritical regime. In particular, this could help fixing the location of the boundary of the decodable region for certain families of graph-based quantum CSS codes in the weak-noise limit.

Finally, is there a numerical method to calculate p_{c} (or p_G) based on finite graph data which works well for euclidean, hyperbolic and random graphs? The crossing point of the cluster sizes gives good results for euclidean and random graphs, but not hyperbolic graphs. The finite size scaling of the largest cluster size works well for hyperbolic graphs and random graphs, but not euclidean graphs.

Data Availability

The data that supports the findings of this study are available at GitHub at `https://github.com/QEC-pages/Homology-changing-percolation-transitions-on-finite-graphs`. The programs used to generate the data and associated scripts are available from the corresponding author upon reasonable request.

Bibliography

[1] M. Aizenman, H. Kesten, and C. M. Newman. Uniqueness of the infinite cluster and continuity of connectivity functions for short and long range percolation. *Comm. Math. Phys.*, 111(4):505–531, 1987.

[2] T. Antunović and I. Veselić. Sharpness of the phase transition and exponential decay of the subcritical cluster size for percolation on quasi-transitive graphs. *Journal of Statistical Physics*, 130(5):983–1009, 2008.

[3] Itai Benjamini, Asaf Nachmias, and Yuval Peres. Is the critical percolation probability local? *Probability Theory and Related Fields*, 149(1):261–269, Feb 2011.

[4] Itai Benjamini and Oded Schramm. Percolation beyond Z^d, many questions and a few answers. *Electronic Communications in Probability*, 1:71–82, 1996.

[5] Charles H. Bennett, David P. DiVincenzo, and John A. Smolin. Capacities of quantum erasure channels. *Phys. Rev. Lett.*, 78:3217–3220, Apr 1997.

[6] Omer Bobrowski and Primoz Skraba. Homological percolation: The formation of giant k-cycles. unpublished, 2020.

[7] S. B. Bravyi and A. Yu. Kitaev. Quantum codes on a lattice with boundary. unpublished, 1998.

[8] N. P. Breuckmann and B. M. Terhal. Constructions and noise threshold of hyperbolic surface codes. *IEEE Transactions on Information Theory*, 62(6):3731–3744, 2016.

[9] Nikolas P. Breuckmann. *Homological Quantum Codes Beyond the Toric Code*. PhD thesis, RWTH Aachen University, 2017.

[10] R. M. Burton and M. Keane. Density and uniqueness in percolation. *Comm. Math. Phys.*, 121(3):501–505, 1989.

[11] A. R. Calderbank and P. W. Shor. Good quantum error-correcting codes exist. *Phys. Rev. A*, 54(2):1098–1105, Aug 1996.

[12] C. R. da Silva, M. L. Lyra, and G. M. Viswanathan. Largest and second largest cluster statistics at the percolation threshold of hypercubic lattices. *Phys. Rev. E*, 66:056107, Nov 2002.

[13] N. Delfosse, P. Iyer, and D. Poulin. Generalized surface codes and packing of logical qubits. unpublished, 2016.

[14] N. Delfosse and G. Zémor. Quantum erasure-correcting codes and percolation on regular tilings of the hyperbolic plane. In *Information Theory Workshop (ITW), 2010 IEEE*, pages 1–5, Aug 2010.

[15] N. Delfosse and G. Zémor. Upper bounds on the rate of low density stabilizer codes for the quantum erasure channel. *Quantum Info. Comput.*, 13(9-10):793–826, September 2013.

[16] N. Delfosse and G. Zémor. A homological upper bound on critical probabilities for hyperbolic percolation. *Ann. Inst. Henri Poincaré Comb. Phys. Interact.*, 3:139–161, 2016.

[17] E. Dennis, A. Kitaev, A. Landahl, and J. Preskill. Topological quantum memory. *J. Math. Phys.*, 43:4452, 2002.

[18] I. Dumer, A. A. Kovalev, and L. P. Pryadko. Numerical techniques for finding the distances of quantum codes. In *Information Theory Proceedings (ISIT), 2014 IEEE International Symposium on*, pages 1086–1090, Honolulu, HI, June 2014. IEEE.

[19] I. Dumer, A. A. Kovalev, and L. P. Pryadko. Thresholds for correcting errors, erasures, and faulty syndrome measurements in degenerate quantum codes. *Phys. Rev. Lett.*, 115:050502, Jul 2015.

[20] I. Dumer, A. A. Kovalev, and L. P. Pryadko. Distance verification for classical and quantum LDPC codes. *IEEE Trans. Inf. Th.*, 63(7):4675–4686, July 2017.

[21] Jingfang Fan, Maoxin Liu, Liangsheng Li, and Xiaosong Chen. Continuous percolation phase transitions of random networks under a generalized achlioptas process. *Phys. Rev. E*, 85:061110, Jun 2012.

[22] M. H. Freedman and D. A. Meyer. Projective plane and planar quantum codes. *Foundations of Computational Mathematics*, 1:325–332, 2001.

[23] Keisuke Fujii and Yuuki Tokunaga. Error and loss tolerances of surface codes with general lattice structures. *Phys. Rev. A*, 86:020303, Aug 2012.

[24] The GAP Group. *GAP – Groups, Algorithms, and Programming, Version 4.8.10*, 2018.

[25] Daniel Gottesman. Theory of fault-tolerant quantum computation. *Phys. Rev. A*, 57:127–137, Jan 1998.

[26] Geoffrey R. Grimmett. *Percolation*, volume 312 of *Grundlehren der mathematischen Wissenschaften*. Springer-Verlag, Berlin Heidelberg, 1999.

[27] Olle Häggström and Johan Jonasson. Uniqueness and non-uniqueness in percolation theory. *Probability Surveys*, 3:289–344, 2006.

[28] Jonathan Hermon and Tom Hutchcroft. Supercritical percolation on nonamenable graphs: Isoperimetry, analyticity, and exponential decay of the cluster size distribution. unpublished, 2019.

[29] Markus Heydenreich and Remco van der Hofstad. *Progress in High- Dimensional Percolation and Random Graphs*. CRM Short Courses. Springer International Publishing, Switzerland, 2017.

[30] Tom Hutchcroft. New critical exponent inequalities for percolation and the random cluster model. unpublished, 2019.

[31] Tom Hutchcroft. Percolation on hyperbolic graphs. *Geometric and Functional Analysis*, 29:766–810, 2019.

[32] Yi Jiang, Ilya Dumer, A. A. Kovalev, and L. P. Pryadko. Duality and free energy analyticity bounds for few-body Ising models with extensive homology rank. *Journal of Mathematical Physics*, 60(8):083302, 2019.

[33] H. G. Katzgraber, H. Bombin, and M. A. Martin-Delgado. Error threshold for color codes and random three-body Ising models. *Phys. Rev. Lett.*, 103:090501, Aug 2009.

[34] Harry Kesten. Some highlights of percolation. In *Proceedings of the International Congress of Mathematitians*, volume 1, pages 345–365, Beijing, 2002.

[35] A. Yu. Kitaev. Fault-tolerant quantum computation by anyons. *Ann. Phys.*, 303:2, 2003.

[36] E. Knill. Scalable quantum computing in the presence of large detected-error rates. *Phys. Rev. A*, 71:042322, Apr 2005.

[37] A. A. Kovalev and L. P. Pryadko. Spin glass reflection of the decoding transition for quantum error-correcting codes. *Quantum Inf. & Comp.*, 15:0825, 2015.

[38] Gady Kozma and Asaf Nachmias. A note about critical percolation on finite graphs. unpublished.

[39] Michael Krivelevich, Eyal Lubetzky, and Benny Sudakov. Asymptotics in percolation on high-girth expanders. unpublished.

[40] Aleksander Kubica, Michael E. Beverland, Fernando Brandao, John Preskill, and Krysta M. Svore. Three-dimensional color code thresholds via statistical-mechanical mapping. unpublished, 2017.

[41] F. J. MacWilliams and N. J. A. Sloane. *The Theory of Error-Correcting Codes*. North-Holland, Amsterdam, 1981.

[42] A. Margolina, H. J. Herrmann, and D. Stauffer. Size of largest and second largest cluster in random percolation. *Physics Letters A*, 93(2):73 – 75, 1982.

[43] M. V. Menshikov. Coincidence of critical points in percolation problems. *Soviet Mathematics, Doklady*, 33:856–859, 1986.

[44] M. V. Men'shikov and A. F. Sidorenko. The coincidence of critical points in Poisson percolation models. *Theory of Probability & Its Applications*, 32(3):547–550, 1988.

[45] Stephan Mertens and Cristopher Moore. Percolation thresholds in hyperbolic lattices. *Phys. Rev. E*, 96:042116, Oct 2017.

[46] M. E. J. Newman and R. M. Ziff. Fast monte carlo algorithm for site or bond percolation. *Phys. Rev. E*, 64:016706, Jun 2001.

[47] F. Sausset and G. Tarjus. Periodic boundary conditions on the pseudosphere. *Journal of Physics A: Mathematical and Theoretical*, 40(43):12873, 2007.

[48] P. W. Shor. Fault-tolerant quantum computation. In *Proc. 37th Ann. Symp. on Fundamentals of Comp. Sci.*, pages 56–65, Los Alamitos, 1996. IEEE, IEEE Comp. Soc. Press.

[49] Jozef Širáň. Triangle group representations and constructions of regular maps. *Proceedings of the London Mathematical Society*, 82(3):513–532, 2001.

[50] Thomas M. Stace, Sean D. Barrett, and Andrew C. Doherty. Thresholds for topological codes in the presence of loss. *Phys. Rev. Lett.*, 102:200501, 2009.

[51] A. M. Steane. Simple quantum error-correcting codes. *Phys. Rev. A*, 54:4741–4751, 1996.

[52] A. M. Steane. Active stabilization, quantum computation, and quantum state synthesis. *Phys. Rev. Lett.*, 78:2252–2255, Mar 1997.

[53] M. F. Sykes and J. W. Essam. Critical percolation probabilities by series methods. *Phys. Rev.*, 133:A310–A315, Jan 1964.

[54] Pengfei Tang. Heavy Bernoulli-percolation clusters are indistinguishable. *Ann. Probab.*, 47:4077–4115, 2019.

[55] R. van der Hofstad. Percolation and random graphs. In Ilya Molchanov and Wilfrid Kendall, editors, *New Perspectives on Stochastic Geometry*, chapter 6, pages 173–247. Oxford University Press, 2010. ISBN 978-0-19-923257-4.

[56] David Wilkinson and Jorge F Willemsen. Invasion percolation: a new form of percolation theory. *Journal of Physics A: Mathematical and General*, 16(14):3365, 1983.

[57] G. Zémor. On Cayley graphs, surface codes, and the limits of homological coding for quantum error correction. In Y. M. Chee, C. Li, S. Ling, H. Wang, and C. Xing, editors, *Coding and Cryptology: Second International Workshop, IWCC 2009, Proc.*, pages 259–273. Springer, Berlin, Heidelberg, 2009.